

CHARACTERIZATION OF MIXED MODEL MEMBRANES OF CATIONIC AND ZWITTERIONIC LIPIDS

— interactions with biological macromolecules

MATTI SÄILY

Helsinki Biophysics & Biomembrane Group

Institute of Biomedicine

Biomedicum Helsinki

University of Helsinki

Finland

ACADEMIC DISSERTATION

To be presented with the assent of the Faculty of Medicine of the University of Helsinki
for public examination in the Small Lecture hall BM LS II of Biomedicum,
Haartmaninkatu 8, Helsinki on 27th January, at noon.
Helsinki 2006

Supervisor: Professor PAAVO KINNUNEN
Helsinki Biophysics & Biomembrane Group
Institute of Biomedicine/Biochemistry
University of Helsinki
Helsinki, Finland

Reviewers: Docent PETER MATTJUS
Department of Biochemistry and Pharmacy
Åbo Akademi University
Turku, Finland

Docent GERHARD GRÖBNER
Biophysical Chemistry
University of Umeå
Umeå, Sweden

Opponent: Docent TOMMY NYLANDER
Physical Chemistry
University of Lund
Lund, Sweden

ISBN 952-91-9739-X (paperback)

ISBN 952-10-2849-1 (PDF)

Helsinki 2005

Yliopistopaino

To Leena

CONTENTS

LIST OF ORIGINAL PUBLICATIONS	7
ABBREVIATIONS	8
ABSTRACT	10
1. INTRODUCTION	12
2. REVIEW OF THE LITERATURE	14
2.1. OVERVIEW OF CELLULAR MEMBRANES AND MEMBRANE MODELS	14
2.1.1. CELLULAR MEMBRANES	
<i>Composition</i>	15
<i>Membranous organelles</i>	15
2.1.2. GENERAL PROPERTIES OF LIPID BILAYERS	16
<i>Effective shapes of lipids</i>	16
<i>Thermotropic phase behavior</i>	17
<i>Pressure profile in bilayers</i>	19
2.1.3. MODEL MEMBRANES	20
<i>Monolayers</i>	20
<i>Liposomes</i>	23
2.2. CHARGED LIPIDS AND MACROMOLECULES	24
2.2.1. CATIONIC LIPIDS	24
<i>Oleamide</i>	24
<i>Sphingosine</i>	24
<i>Gemini surfactants</i>	25
2.2.2. LIPID-DNA INTERACTIONS	25
<i>Interactions in air-water interface</i>	25
<i>Implications for gene therapy</i>	26
2.2.3. LIPIDS AND PROTEINS INTERACTING	27
3. OUTLINE OF THE PRESENT STUDY	29
4. MATERIALS AND METHODS	30
4.1 MATERIALS	30
4.2 METHODS	31
4.2.1. COMPRESSION ISOTHERMS (I, II, IV)	31
4.2.2. DIFFERENTIAL SCANNING CALORIMETRY (III, IV)	31
4.2.3. LIGHT SCATTERING (III, IV)	32
4.2.4. RESONANCE ENERGY TRANSFER (III)	32
4.2.5. DETECTION OF THE CLEAVAGE OF DSP ON MONOLAYERS (IV)	32
4.2.6. SURFACE PLASMON RESONANCE (IV)	32
4.2.7. DETERMINATION OF CMC (IV)	33
4.5.8. STUDIES ON GIANT VESICLES (IV)	33

5. RESULTS	35
5.1. MIXED MONOLAYERS OF POPC AND CATIONIC LIPIDS (I + II)	
5.1.1. CHARACTERIZATION OF MIXED MONOLAYERS OF POPC AND DHAB: EFFECTS OF DNA	35
<i>Compression isotherms</i>	35
<i>Effects of DNA</i>	36
<i>Monolayer compressibility modulus</i>	37
5.1.2. SPHINGOSINE-PHOSPHATIDYLCHOLINE MONOLAYERS: EFFECTS OF DNA	39
<i>Force-area isotherms for sphingosine/POPC monolayers</i>	39
<i>Effects of DNA</i>	39
<i>Changes in monolayer dipole potential ψ</i>	42
<i>Excess free energy of mixing</i>	42
5.2. LIPID PROTEIN INTERACTIONS (III)	45
<i>Light scattering</i>	45
<i>Resonance energy transfer</i>	46
<i>Time course of the binding</i>	47
<i>Differential scanning calorimetry</i>	47
5.3. REDUCTIVE CLEAVAGE OF DISULFIDE BOND CONTAINING CATIONIC GEMINI SURFACTANT IN MONOLAYERS AND IN BILAYERS (IV)	50
<i>CMC</i>	50
<i>Differential scanning calorimetry</i>	51
<i>Monolayer experiments</i>	51
<i>SPR experiments</i>	52
<i>Studies with GUVs and LUVs</i>	53
6. DISCUSSION	55
6.1. MIXING FAR FROM IDEAL: monolayers of POPC and DHAB(I) or SPH(II)	55
6.1.1 REORIENTATION OF THE PHOSPHOCHOLINE DIPOLE	56
6.1.2. A HIGHLY SENSITIVE MOLE FRACTION DEPENDENT MIXING	58
6.1.3. SURFACE DIPOLE POTENTIAL	60
6.2. THE INTERACTIONS OF MEMBRANES AND CHARGED MACROMOLECULES	62
6.2.1. INTERACTION OF DNA WITH CHARGED MONOLAYERS	62
6.2.2. THE INTERACTION OF PROTEIN P17 WITH POSITIVELY CHARGED LIPID MEMBRANES	63
6.3. REDUCTIVE CLEAVAGE OF A GEMINI SURFACTANT: IMPLICATIONS FOR GENE DELIVERY	64
7. ACKNOWLEDGEMENTS	66
8. REFERENCES	68
ORIGINAL PUBLICATIONS	

...If a drop of oil is put on a polished marble table, or on a looking glass that lies horizontally; the drop remains in place, spreading very little. But when put on water it spreads instantly many feet round, becoming so thin as to produce prismatic colors, for a considerable space, and beyond them so much thinner as to be invisible, except in its effect of smoothing the waves at a much greater distance.

(B. Franklin, 1774)

ORIGINAL PUBLICATIONS

This thesis is based on the following original publications, referred to in the text by Roman numerals I-IV.

I. V. Matti J. Säily, Samppa J. Ryhänen, Juha M. Holopainen, Stefano Borocci, Giovanna Mancini, and Paavo K. J. Kinnunen. "Characterization of mixed monolayers of phosphatidylcholine and a novel dicationic gemini surfactant SS-1 with a Langmuir balance: effects of DNA." *Biophys. J.* 2001. 81: 2135-2143.*

II. V. Matti J. Säily, Juha-Matti Alakoskela, Samppa J. Ryhänen, Mikko Karttunen, and Paavo K. J. Kinnunen. "Characterization of Sphingosine—Phosphatidylcholine Monolayers: Effects of DNA." *Langmuir* 2003. 19: 8956-8963.

III. Juha M. Holopainen, Matti Säily, Javier Caldentey, and Paavo K. J. Kinnunen "The assembly factor P17 from bacteriophage PRD1 interacts with positively charged lipid membranes." *Eur J Biochem.* 2000. 267:631-6238.

IV. V. Matti J. Säily, Samppa J. Ryhänen, Hilikka Lankinen, Paola Luciani, Giovanna Mancini, Mikko J. Parry, and Paavo K. J. Kinnunen. "Impact of Reductive Cleavage of an Intramolecular Disulfide Bond Containing Cationic Gemini Surfactant in Monolayers and Bilayers." *Langmuir*, *in press*.

Publication I will also be used as a part of dissertation of MD Samppa Ryhänen.

*Erratum considering the structure of the surfactant used in original publication I was published in *Biophys. J.* 2005. 89: 753 (see original publications section). Corrected structure and nomenclature described in erratum is used throughout this thesis.

ABBREVIATIONS

A	area per molecule
A_{DNA}	area per molecule recorded with DNA in the subphase
A_{L}	lift-off area
CL	cationic lipid
CMC	critical micellar concentration
C_{S}^{-1}	elastic modulus of area compressibility
DHAB	<i>N,N</i> -dimethyl- <i>N,N</i> -dihexadecyl ammonium bromide
DMPC	1,2-dimyristoyl- <i>sn</i> -glycero-3-phosphocholine
DPPE	1,2-dipalmitoyl- <i>sn</i> -glycero-3-phosphatidylethanolamine
DOG	dioleoylglycerol
DSC	differential scanning calorimetry
DSP	<i>N,N</i> -dimethyl- <i>N</i> -hexadecyl- <i>N</i> -(2-{2-[<i>N,N</i> -dimethyl- <i>N</i> -hexadecylammonio]ethyl}dithio)ethyl ammonium dibromide
F-DPPE	<i>N</i> -(fluorescein-5-thiocarbonyl)-1,2-dipalmitoylphosphatidyl-ethanolamine
GSH	glutathione
GUV	giant unilamellar vesicle
L_{α}	fluid phase
L_{β}	gel phase
LE	liquid expanded state
LC	liquid condensed state
LS	light scattering
LUV	large unilamellar vesicle
MLV	multilamellar vesicle
MSP	[<i>N,N</i> -dimethyl- <i>N</i> -hexadecylammonio]ethylthiol bromide
NMR	nuclear magnetic resonance
P_{β}	ripple phase
PC	phosphatidylcholine or personal computer depending on context
PE	phosphatidylethanolamine
PI	phosphatidylinositol

POPC	1-palmitoyl-2-oleoyl- <i>sn</i> -glycero-3-phosphocholine
POPG	1-palmitoyl-2-oleoyl- <i>sn</i> -glycero-3-phosphatidylglycerol
PS	phosphatidylserine
RET	resonance energy transfer
RFI	relative fluorescence intensity
RI	relative intensity
R-P17	rhodamine-P17
SM	sphingomyelin
SOPC	1-stearoyl-2oleoyl- <i>sn</i> -glycero-3-phosphocholine
Sph	sphingosine
SPR	surface plasmon resonance
SUV	small unilamellar vesicle
TLC	thin layer chromatography
T _m	main transition temperature
X _A	mole fraction of compound A
ΔG_m^{ex}	excess free energy of mixing
ΔH	enthalpy
π	surface pressure
ψ	dipole potential

ABSTRACT

Biomembranes divide the cellular spaces and, moreover, actively take part in cellular functions as receptors and second messengers, for example. Different membranes contain a strictly controlled and varying pattern of charged lipids and many biologically significant macromolecules possess charges that have a drastic influence on their interplay with the cellular context.

The present study focuses on the physicochemical properties of charged membranes and their interactions with charged macromolecules. In brief, the results showed that even small amounts ($< 5\%$) of the naturally occurring cationic lipid sphingosine as well as a synthetic positively charged lipid, DHAB, strongly condense phosphatidylcholine monolayers. This effect is suggested to reflect reorientation of the $P^+ N^+$ dipole of the PC headgroup in keeping with a simultaneous increase in surface dipole potential Ψ . Mixed monolayers of sphingosine and POPC showed an intriguing behavior. Three critical mole fractions X_{Sph} of sphingosine, viz., 0.25, 0.6, and 0.83, were observed at which the area/molecule reached a local minimum followed by a pronounced expansion of the film. This suggests energetically favorable ordering allowing the positively charged sphingosines to maximize their distance, so as to minimize the coulombic repulsion. It is possible that sphingosine and POPC segregate laterally as a regular lattice.

The interplay of charged macromolecules with membranes is of great biological significance. The physical state and the composition of the membrane lipids is crucial for the functioning of several integral and peripheral proteins. On the other hand the interactions of cationic surfactants and DNA are of special interest because of their use in gene transfection. Naturally occurring sphingosine is suggested to contribute to the control of DNA replication and gene expression via electrostatic attraction. To this end, the presence of DNA affected the mixed DHAB/POPC films differently depending on the constituent lipid stoichiometry as well as on the DNA/DHAB charge ratio. Interestingly, DNA condensed neat POPC monolayers and at $X_{\text{DHAB}} > 0.5$ an expansion due to DNA

was evident. The avidity of the assembly factor P17 from bacteriophage PRD1 to positively charged vesicles containing sphingosine was observed by calorimetry, light scattering, and resonance energy transfer suggesting that P17 might contribute to the morphogenesis of PRD1 via electrostatic membrane-related interactions.

Our studies on a reducible cationic gemini surfactant DSP revealed effective cleavage of the disulfide bridge in the lipid spacer induced by glutathione both in monolayers and in vesicles. In Langmuir monolayers the reductive cleavage led to a decrease in surface pressure π as well as surface dipole potential Ψ , and in giant vesicles a disruption of the GV during a period of approx. 30 s was observed. In the presence of a charge saturating concentration of DNA the process attenuated but, importantly, DNA did not prevent the reduction. Moreover, the resulting monomers had significantly less affinity towards DNA in supported monolayers. The above results provide evidence that this surfactant could well be suitable for transfection *in vivo*.

1. INTRODUCTION

The motivation for this study arised from the enormous diversity of lipids in biological membranes and the plethora of roles they possess in many fundamental biological processes. Our aim was to study the physicochemical basis of lipid mixing, and the interactions that biological macromolecules have with the membranes. More specifically, we characterized mixed monolayers of cationic and zwitterionic lipids, studied their interactions with DNA and protein, and examined the membrane properties of an reducible cationic amphiphile and observed the effects of its cleavage. Due to the inherent complexity of biological membranes we used model membranes, namely monolayers and vesicles, in our studies.

Lipids form, together with DNA and RNA, proteins, and carbohydrates, the basic building blocks required for life. For decades the lipid membranes were considered merely as a passive framework enabling the actions of proteins but these views have changed to a much more elaborate and fascinating direction. Lipids function as second messengers, regulators of gene expression, enzymes, and receptors ¹⁻⁴. The spectrum of diseases related to lipid metabolism ranges from atherosclerosis ⁵ to psychiatric illnesses ⁶. Furthermore, the accessibility to certain lipids has been claimed to be associated with the evolution of modern hominid brain ⁷.

Lipid bilayers are truly dynamic, fluid, and complex structures composing of lipids, proteins, and carbohydrates. The fluid mosaic model ⁸ introduced the fluidity of the bilayer but missed the principle characteristics of membranes as nonrandom, laterally heterogeneous assemblies that contain compositionally distinct domains and compartments ⁹. Membranes are sensitive to both physical and chemical factors and thus provide exceptional mediator for biological triggering and signaling processes.

Peripheral membrane interactions play a crucial role in regulating several fundamental cellular functions. The physical state of the lipids in the membranes influence the functioning of proteins and vice versa ¹⁰⁻¹³. In addition to interacting with proteins lipids

have interactions with DNA. The latter are of great importance due to the growing interest towards liposomal gene transfection^{14, 15}. The potential of gene therapy is well documented but the lack of efficient and safe transfection vectors restricts its wider use¹⁶⁻¹⁸. Basic research of the physicochemical forces and interactions involved in the complex formation between lipids and DNA is essential in developing future vehicles. Moreover, the above interactions share also a wider biological significance since the naturally occurring cationic lipid sphingosine is known to contribute to regulation of gene expression and the control of replication^{3, 19}.

I will briefly overview the cellular membranes and the model membranes used for studying them in the following literature review. In addition, the interactions of charged membranes with macromolecules are discussed. This will be followed by the outline of the present study and thereafter with results and discussion. The main focus will be on cationic lipids interacting with zwitterionic phosphatidylcholines, and on the other hand with either DNA or protein. Acknowledgements, references and the original publications (I-IV) are presented as a last part of this thesis.

2. REVIEW OF THE LITERATURE

2.1. OVERVIEW OF CELLULAR MEMBRANES AND MEMBRANE MODELS

Eukaryotic cells contain over 1000 different lipid species and, moreover, cells actively regulate their lipid composition ²⁰. In addition to forming biological membranes, lipids serve as energy storage, enzyme cofactors, hydrophobic anchors, emulsifying agents, hormones, and intracellular messengers ²¹. Owing to these wide functions of great importance it has been proposed that after decades of proteins and genes one should get ready for the decade of the lipids ²².

2.1.1. Cellular membranes

In 1925 the first important step towards understanding biological membranes was taken as the membrane of red blood cells was shown to be only two molecules thick ²³. The membranes were emphasized as fluid and randomly distributed structures by Singer and Nicholson in their fluid-mosaic model ⁸. Thereafter proteins and sugars have been included into the models, and the general view of the nature of the membranes has evolved towards heterogeneous, non-randomly compartmentalized bilayers where dynamics plays a decisive role (Fig. 2.1.) ^{9, 24, 25}. Lipid molecules in lipid bilayers can change their conformation, rotate around their molecular axis, diffuse laterally, protrude out of bilayer plane, and flip-flop between the two monolayers ⁹. Despite fluid dynamics local structuring and order takes place. Sphingolipids and cholesterol, for example, have been shown to enrich in domains ²⁶⁻²⁸ to which certain proteins attach.

Composition

Eukaryotic plasma membranes share the same lipid species and generally include PE, PC, PI, PS, SM, cholesterol and a small fraction of other lipids like two negative charges possessing cardiolipin²⁹. Phospholipids are asymmetrically distributed between the inner and outer monolayer of plasma membrane. Neutral phosphatidylcholine and sphingomyelin are found merely in the outer, and phosphatidylethanolamine in the inner monolayer. Negatively charged phosphatidylserine, phosphatidylinositol and phosphatidic acid are primarily located in the inner cytosolic monolayer²¹. Integral and peripheral proteins are embedded in the lipid bilayer and together with lipids and carbohydrates they form a characteristic pattern with locally enriched lipids floating as domains on the membrane (Fig. 2.1.).

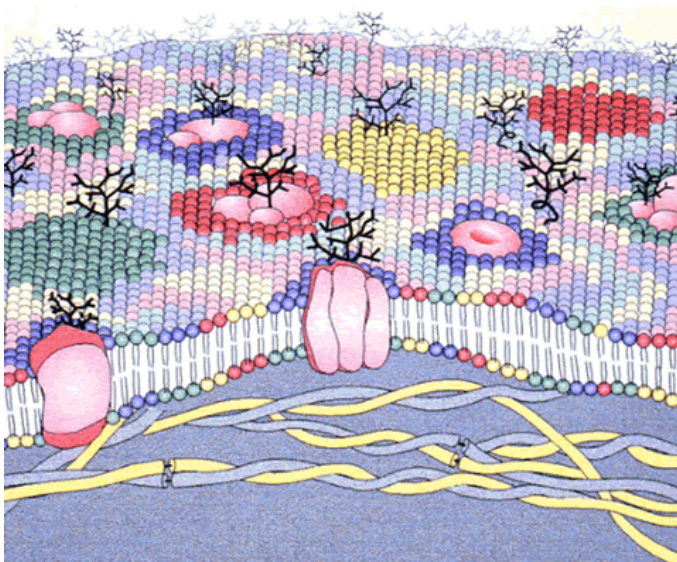


Figure 2.1. A schematic representation of plasma membrane. (reproduced with permission of HBBG).

Membranous organelles

Membranes define the external boundaries of cells as well as divide their internal space into compartments. In addition to structural role, membranes also determine the nature of all communication between the inside and outside of a cell. Moreover, most of the fundamental biochemical processes, such as DNA replication, protein biosynthesis, protein secretion, bioenergetics, and hormonal responses, involve membranes. Eukaryotic cells have a multitude of membranous organelles differing in composition, structure, and

function²⁹. The plasma membrane separates the cell from its surroundings and serves at the same time as a contact point between the cell and its environment. The nuclear membrane encloses DNA and defines the nuclear compartment. The endoplasmic reticulum fills about half of the total area of membrane in eukaryotic cells and provides the site for protein synthesis. The Golgi apparatus dispatches lipids and proteins from ER to a variety of destinations. Oxidative phosphorylation takes place in mitochondrion, and lysosomes are responsible for macromolecular degradation. Endosomes and peroxisomes constitute the smallest compartments, occupying approx. one percent of the total cell volume³⁰. All of the above membranous organelles serve specialized functions, but still share basic properties that define the universal behavior of biomembranes. They are, for example, able to self-seal, flex, and to be selectively permeable²¹.

2.1.2. General properties of lipid bilayers

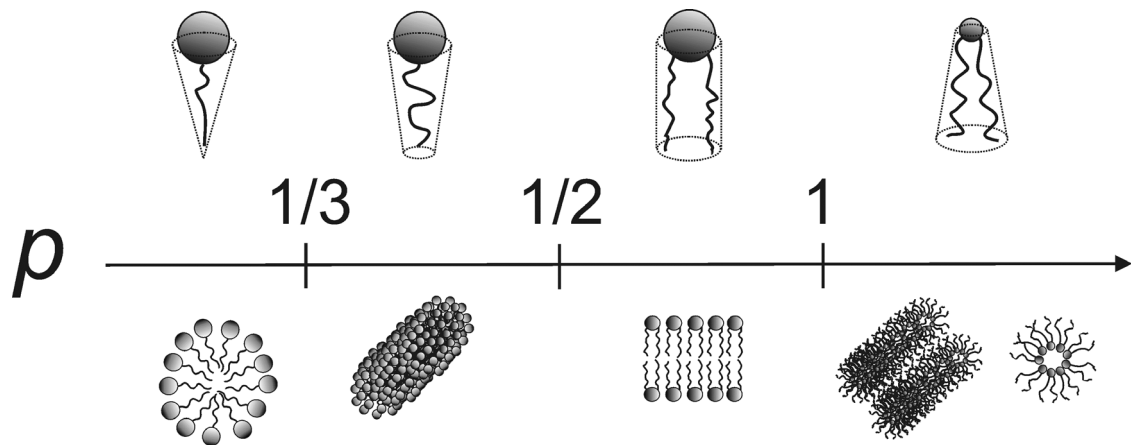
Lipids self-assemble into membranes due to their amphiphilic nature. Hydrophobic interactions among lipid molecules provide the driving force for membrane formation: the polar headgroup is hydrated and the hydrophobic acyl chains point away from the aqueous solvent. The fundamental properties of membranes include that the lipids are not linked by strong chemical forces but are, instead, kept together by weak and noncovalent interactions. This allows the membranes to be soft, a property required for various modes of their principal functions⁹.

Effective shapes of lipids

The effective shape of a lipid molecule defines the shape of the membrane structure it forms³¹ and variations in pH and counterion concentration have been shown to contribute to lipid packing by altering polar headgroup hydration, headgroup-water interactions, and the strength of hydrogen bonding between adjacent polar headgroups. The effective molecular shape is conveniently described by packing parameter P ³²,

$$P = v/(a \times l),$$

where v = the effective volume of the hydrophobic part of the molecule, a = the limiting surface area of its hydrophilic part, and l = the length of its hydrophobic part. The impact of the effective shape as a function of packing parameter P with the corresponding aggregates is illustrated in Fig. 2.2.



Lysophospholipids (sphingosine etc.)	PC, SM, PS, PI,	PE, cholesterol
Detergents	PG, PA	

Figure 2.2. Schematic illustration of different effective shapes of lipid molecules forming aggregates with varying structures. $P < 1/3$ yields spherical micelles, $1/3 < P < 1/2$ rodlike micelles, $1/2 < P < 1$ lamellar bilayers, and $P > 1$ results in inverted hexagonal bilayer and finally inverted micelles. (Drawn by S.J. Rvhänen)

Thermotropic phase behavior

Lipid membranes can undergo phase transitions with different phases reflecting different degrees of order^{9, 29}. The best characterized transition for phospholipids is the main transition from the rippled gel-like P_{β} phase to the fluidlike phase L_{α} . L_{α} phase is disordered, with extensive rotational motion of the headgroups and increased lateral diffusion of the whole molecule. P_{β} phase represents an intermediate between the fluid

and gel phases and it has recently been proposed that domains of gel-like interdigitated phase and disordered liquid phase co-exist in P_{β} .³³ In gel phase (L_{β}) the acyl-chains are ordered and the lipid molecules are arranged in a regular structure. Changes in the phase state induce dramatic changes in the properties of the bilayers, such as elastic moduli³⁴⁻³⁶. Biological membranes largely remain in the fluid phase state but within the membranes local domains with varying phases exist due to interactions between different lipids as well as membrane proteins⁹. Phase behavior of lipids has been extensively studied with different model systems, for example differential scanning calorimetry (DSC)(Fig. 2.3.)

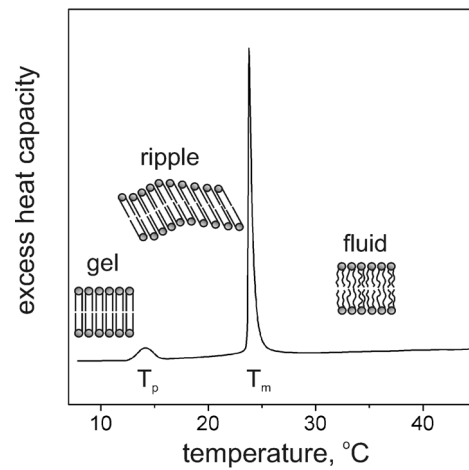


Figure 2.3. A differential calorimetry trace of DMPC multilamellar vesicles with schematic illustrations of different phases. (Drawn by S.J. Ryhänen)

Pressure profile in bilayers

Phospholipid bilayers as well as biological membranes have an internal pressure that results from the amphiphilic nature of the lipids: the hydrophilic headgroups are squeezed together to prevent exposure of the hydrophobic tails to the solvent while simultaneously strong repulsions between the hydrocarbon chain tend to expand the membrane^{37, 38} (Fig 2.4.). As a result the total lateral pressure in the membrane is zero even though the contribution of different components can be of order of several hundred bars. Estimates over the magnitude of the lateral pressure in model and in biomembranes vary but most commonly the value is in the region of 30-35 mN/m³⁷. Variations in the lipid compositions have been suggested to influence the function of membrane bound proteins via changes in membrane lateral pressures¹⁰. According to recent molecular dynamics simulations cholesterol modifies the lateral pressure profile of membranes in a way that might indicate specific pressure mediated interaction between cholesterol and proteins³⁹. It is tempting to speculate, that also steroid hormones could mediate their actions partly via the same mechanism.

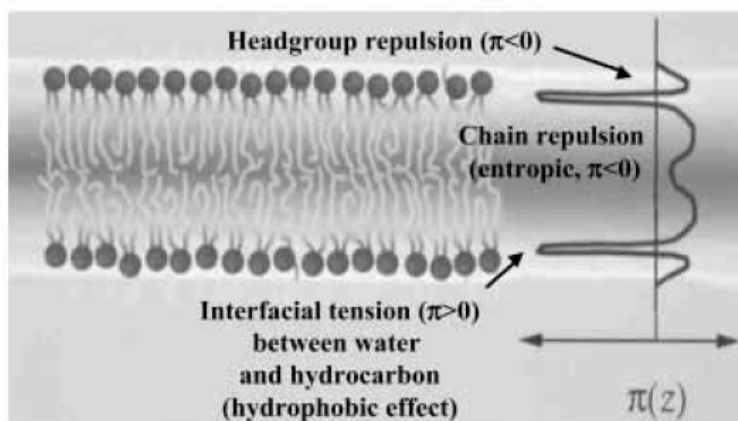


Figure 2.4. Lateral pressure profile of a bilayer. Interfacial tension compensates the repulsion of headgroups and acyl chains. (Kinnunen, 2000)

2.1.3. Model membranes

Direct biophysical research of dynamic and complex biomembranes is demanding and in many cases beyond the reach of present methods. Model membranes, namely lipid monolayers and liposomes, provide simplified and efficient tools for experimentalists.

Monolayers

The first monolayer experiments were performed in 1774 by Benjamin Franklin, who spread a teaspoonful (2 ml) of oil over an area of half acre (approx. 2000 m²) on the surface of a pond⁴⁰. This gave him a film thickness of 2.5 nm but it took over a hundred years, however, to realize that this thickness represents a layer just one molecule thick, i.e. a lipid monolayer. The pioneering work in the physics of surface films at air-water interface was performed in a kitchen sink, when surface contamination as a function of area for different oils was determined⁴¹. First systematic studies on monolayers on air-water interface were performed by Irving Langmuir in the late 1910's and early 1920's⁴². Langmuir monolayer refers nowadays simply to the insoluble monomolecular film on the surface of a liquid. The studies by Langmuir were further complemented by Katherine Blodgett⁴³ and therefore the monolayer assemblies on solid supports, transferred layer-by-layer from the water surface, are called Langmuir-Blodgett films.

Langmuir films present several advantages compared to bilayers. The interactions of interest are confined within a two-dimensional layer, thus avoiding the mesophasic structural changes often occurring in other model membranes⁴⁴. Measurements of the surface pressure–area (π -A) isotherms give information on the intermolecular interactions that are not accessible directly from bilayers³⁷. Moreover, lipid-lipid interactions in a range of molecular areas known to occur in the membrane can be investigated in a systematic manner, with π -A isotherms and compressibility providing precise indicators of changes in the film structure⁴⁴. The onset and completion pressures of phase transitions can be further determined by examining the elastic moduli of area compressibility C_S^{-1} as a function of pressure⁴⁵. The electrical potentials that arise from

dipoles both in the lipid molecule and those in the water of lipid hydration can be directly measured across the lipid monolayer ⁴⁶.

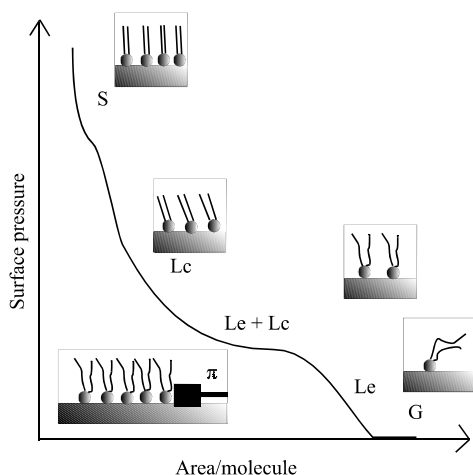


Figure 2.5. A Langmuir film deposited on air-water interface. A schematic illustration of a force-area isotherm with indications for respective phases is given (see text for details). In the bottom a cut through a Langmuir through, where area and pressure can be varied by moving the barrier.

Lipids with different kind of acyl-chains and different headgroups occupy different areas. These areas can be determined from π -A isotherms where the particular collapse pressure represents a point at which the molecules are packed to their maximum density. The minimum surface area for a disaturated phospholipid, DMPC for example, is around 45 \AA^2 and for an unsaturated lipid, such as POPC, it is close to 60 \AA^2 . Discontinuities in force-area isotherms indicate structural phase transitions ⁴⁷ (Fig. 2.5.). The very dilute monolayer, with an area of hundreds of $\text{\AA}^2/\text{molecule}$, is described as two-dimensional gas (G). With increasing pressure, i.e. decreasing area/molecule, the monolayer enters the liquid expanded phase (LE). The heads and the tails of the lipids are assumed to be disordered in both G and LE but, however, X-ray data reveal some crystallinity also in the uncompressed state indicating coexistence of crystalline solid with disordered phase ⁴⁸. Further compressing the monolayer results in a transition from LE to liquid condensed phase (LC) with a plateau indicating first order transition. The plateau is, however, not always horizontal and this is explained by the formation of small molecular aggregates or surface micelles ⁴⁹. Yet another kink can be observed upon compression of the monolayer and traditionally this refers to transition from LC to solid phase (S). Recent X-ray studies show that the transition is in the level of the orientation of the chains with respect to the

water surface from tilted in LC to perpendicular in S⁴⁹ and that the monolayer in fact possesses same degree of translational order in both regions. Major differences arise in the lateral compressibility so that in the tilted LC state the monolayer is relatively easily compressible with the decrease in area/molecule achieved by decrease in the tilt angle. In untilted (S) phase the molecules are much more closely packed and thus less compressible. The co-existence of two phases within the same monolayer can be illustrated by fluorescence microscopy⁵⁰ and very complex patterns can arise as a consequence of line tension of the lipid domains and the electrostatic interaction between domains competing (Fig. 2.6.)⁵¹.

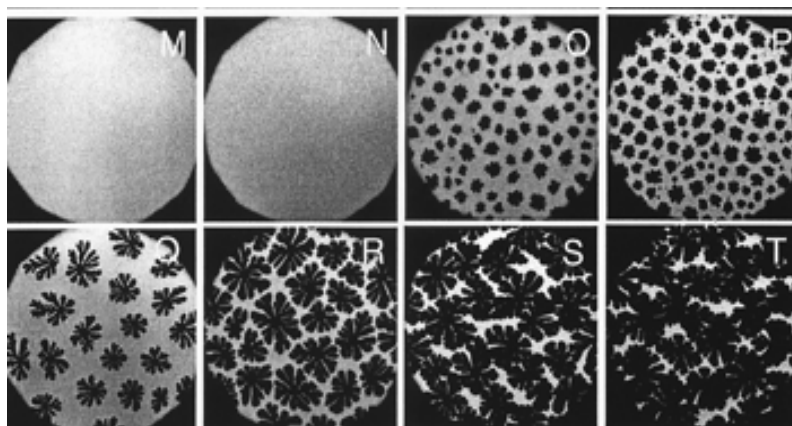


Figure 2.6. Fluorescence microscopy images of a DMPC/C24:1-ceramide/NBD-PC (79:20:1, molar ratio) (*M-P*), and DMPC/C24:1-ceramide/NBD-PC (29:70:1, molar ratio) (*Q-T*), monolayers at surface pressures (from left to right) of 5, 15, 30, and 40 mN/m. (Modified from Holopainen et al 2001)

Nature takes advantage on lipid monolayers for example in the alveoli of lungs⁵². Alveoli are air-filled cavities that are responsible for gas exchange during breathing. Lipid monolayer covers the epithelial surface of an alveolus and its presence lowers the interfacial tension and thus also the Laplace pressure. This prevents the alveoli from collapsing and significantly reduces the work required for inhalation. The lung surfactant is mostly DPPC, while also some PG and cholesterol as well as proteins are present^{53, 54}.

Liposomes

Liposomes, viz. spherical lipid vesicles, with different diameters can be prepared. Small unilamellar vesicles (SUVs) are lamellar lipid bilayers with diameters from 20 to 50 nm, large unilamellar vesicles (LUVs) are usually from 50 to 100 nm, and the diameter of giant unilamellar vesicles (GUVs) usually varies between 10 and 100 μm ^{29, 55, 56} (Fig. 2.7.). The size of a GUV is similar to that of actual cells and thus GUVs provide an interesting model for studies on events occurring in plasma membranes⁵⁷. The actions of different enzymes, such as phospholipase C and sphingomyelinase⁵⁸⁻⁶⁰, as well as other membrane related processes have been studied with GUVs^{60, 61}.

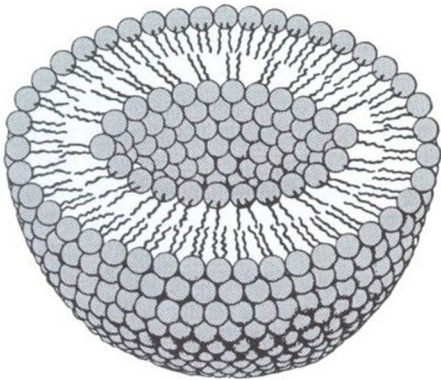


Figure 2.7. A schematic drawing representing half of a lipid vesicle.

2.2. CHARGED LIPIDS AND MACROMOLECULES

The behavior of numerous macromolecules on the membrane surfaces is modified by the type of lipids present⁶² and on the other hand absorbed polyelectrolytes produce changes in the ordering of lipid membranes that reflect to both monolayers, even if they were composed only of single type of phospholipid⁶³. Charge distribution within the membrane, together with complex combination of electrostatic, hydrophobic and entropic effects, is likely to determine the type and extent of the interaction with associated molecules^{9, 62}. In the following chapters the interactions of charged lipids with DNA and proteins are discussed.

2.2.1. Cationic lipids

Oleamide

There are only two naturally occurring cationic lipids, namely sphingosine and sleep inducing lipid oleamide. Oleamide was first found in the cerebrospinal fluid of sleep-deprived cats⁶⁴ and it has been shown to induce cannabimimetic effects⁶⁵ including suppression of pain and inflammation. In addition, oleamide affects GABAergic, dopaminergic, and serotonergic transmission⁶⁶ but the definitive mechanisms for its actions remain obscure⁶⁷.

Sphingosine

Sphingosine, a sphingolipid metabolite, has been shown to modulate diverse cellular functions such as growth and differentiation, initiation and maintenance of various immunological responses, receptor function, and oncogenesis⁶⁸⁻⁷⁰. It has also been shown to increase tone in coronary as well as renal arteries and, to decrease survival after myocardial ischemia^{71, 72}. Sphingosine and other lysosphingolipids are potent and reversible inhibitors of protein kinase C⁶⁸ and a number of other kinases⁷³⁻⁷⁵. It has been suggested that the cationic nature of sphingosine would be crucial in exerting and mediating its diverse functions⁷⁶ and that electrostatically controlled complex formation

of sphingosine with acidic phospholipids may take place in membranes. Moreover, besides introducing a positive surface charge allowing the binding or activation of some proteins, sphingosine could influence membrane-mediated cellular processes by altering the organization and state of membrane lipids ⁷⁷.

Gemini surfactants

Cationic gemini surfactants are composed of a central spacer pairing two identical long chain hydrophobic tails both carrying a cationic headgroup. The basic structure offers possibilities for structural variations and, indeed, extensive screening for compounds having desired physicochemical properties has been carried out ⁷⁸. Gemini surfactants are significantly more surface active than conventional surfactants and they have applications in, for example, disinfection and most importantly in gene transfection ⁷⁹. Including a disulfide bridge into the spacer yields a reducible gemini surfactant ⁸⁰ specially designed for transfection purposes. In addition to the above, unexpected and intriguing behavior of gemini surfactants in salt solutions has been observed varying from self-assembly into cytomimetic structures ⁸¹ to aggregation into crystal-like structures ⁸².

2.2.2. Lipid-DNA interactions

Research on DNA-lipid interactions is motivated by three main lines: (i) need for an efficient and safe non-viral method for gene transfection, (ii) need for drug delivery vehicles in general, and (iii) quest for useful novel materials. Moreover, naturally occurring charged lipids, sphingosine in particular, may have poorly defined interactions with DNA that need to be resolved in order to understand their function.

Interactions in air-water interface

Electrostatic attraction drives the complex formation between cationic lipids and negatively charged phosphates of DNA ^{19, 83, 84}. The presence of DNA results in expanded monolayers indicating interaction and possible intercalation of DNA into the film ^{85, 86}. Moreover, monolayer packing density has been proposed to affect the packing of DNA

⁸⁶. DNA bound to a Langmuir-Blodgett film has recently been enzymatically degraded by DNase ⁸⁷. The length of the spacer of a gemini surfactant seems to play an important role in determining the properties of the monolayers complexed with DNA ⁸⁸. From X-ray diffraction studies it has become evident that DNA starts to adsorb, producing heterogeneous layer, already during dropwise spreading of the amphiphile before any compression ⁸⁹. In the same study the thickness of the absorbed DNA layer to the monolayer (composed of a monocationic lipid) varied from 30 Å at low pressure to 70 Å at high pressure yielding 3 times the amount of DNA necessary for complete lipid charge compensation ⁸⁹. Screening of the charges in DNA by counterions may be responsible for the observed unexpectedly dense packing. Films complexed with DNA had higher compressibility than neat lipid films in keeping with the observation of lateral heterogeneity in lipid distribution resulting from absorbed DNA ^{83, 89, 90}.

Implications for gene therapy

The therapeutic potential of gene transfer has been confirmed with results from some immunodeficiency syndromes ¹⁷ and malignant tumors ¹⁶. However, lack of efficient gene transfection vectors continues to present the major barrier for adapting gene therapy as a routine. Viral vectors were the primary choice for gene therapy but they exhibit severe disadvantages including immunogenicity, difficult production, limited insert size, and biohazards ^{18, 91}. Being relatively easy to prepare and lacking most of the problems associated with viruses, complexes of DNA with cationic liposomes (lipoplexes) are now considered to represent perhaps the most promising vehicle for use in gene therapy ^{14, 15, 92}.

Several properties have been claimed to determine the transfection efficiency of lipoplexes ^{15, 78, 92-94} and multitude of models for the organization of DNA/CL complexes have been suggested ^{95, 96}. It is evident that for optimal transfection *in vivo* a very delicate composition of lipoplex is required ^{14, 15, 78, 84, 92, 94, 97-100}. The amount of cationic lipid, helper lipids, and other ingredients (such as proteins) needs to be adjusted carefully and this tuning of the composition is rather laborious with cell cultures. Moreover, the *in vitro* transfection efficiency does not necessarily correlate to *in vivo* results ¹⁰¹.

In order to study different complexes and to eventually enhance the poor efficiency, model membranes can be used to rationally resolve the basic mechanisms and forces governing the interactions between charged lipids and DNA. Langmuir monolayers enable systematic characterization of mixed lipid films and investigation of the impact of DNA to these systems. However, very few thorough characterizations of such systems have been conducted.

2.2.3. Lipids and proteins interacting

Electrostatic forces, mediated by negatively charged lipid components in the membrane, drive the binding of basic peripheral proteins to their surface¹¹. The binding of proteins induces demixing of the lipid molecules in the membranes and the degree of demixing regulates the binding affinity¹¹. Membrane lipids are extensively and delicately utilized also by specific integral membrane proteins and the action of these proteins appears to be determined by their lipid environment^{20, 102}. The membrane spanning regions of such proteins are highly conserved, implying these regions to have also other functions than just hydrophobic anchoring of the protein into the bilayer. For example, the hydrophobic length of the transmembrane domain influences the bilayer so that possible hydrophobic mismatch leads to sorting of the lipids around the protein¹⁰³ and, moreover, changing the hydrophobic mismatch can trigger the function of integral proteins¹⁰⁴. The selection of accumulated lipids can be varied by changing membrane composition, thermodynamic conditions, or by addition of membrane modifying compounds⁹. Conformational changes in the protein also lead to changes in the content and extent of accumulated lipids. Hydrophobic matching thus links the physical properties of membrane lipids to the functioning of proteins. Furthermore, variations in membrane composition can lead to changes in lateral pressure profile in lipid bilayers and small changes in the lateral pressure, in turn, can induce changes in conformation of integral proteins^{10, 38}. Surface charge of the membranes strongly affects the function of glycolipid transfer protein, that is thought to mediate and maintain a specific distribution of intracellular glycosphingolipids, and thus via certain transfer proteins membranes are able to regulate

their own composition ¹⁰⁵. In addition, electrostatic interactions between histones and DNA can be influenced by sphingosine and acidic phospholipids ¹⁰².

Functional ordering in cellular membranes is proposed to influence the function of proteins and enzymes ^{13, 20}. The action of protein kinase C, a key enzyme in cellular signal transduction, is enhanced by the addition of PE lipids. These lipids, having a small headgroup, exhibit a propensity to form H_{II} phases thus carrying an intrinsic curvature stress in lamellar membranes (see Fig. 2.2.). The binding of PKC is able to partly release this stress by inducing extended chain conformation ¹⁰². Also other membrane active proteins have hydrophobic pockets for extended lipid chains and direct evidence of extended lipid anchorage for cytochrome C, for example, has emerged ¹⁰⁶.

3. OUTLINE OF THE PRESENT STUDY

This study was motivated by the multitude of roles charged lipids have in membranes and, moreover, by increasing interest towards liposomal gene delivery. The interplay between cationic lipids and DNA is surprisingly complex and studies with model membranes are thus needed to widen our understanding of the physicochemical basis governing these interactions. Furthermore, charged membranes provide the scene for action to a large variety of proteins and, accordingly, are in a key position in many fundamental biological events. In keeping with the above, the aims of this study can be divided into three themes, as follows:

- (i) To characterize mixed monolayers of cationic and zwitterionic lipids and their interaction with DNA,
- (ii) To study possible membrane interactions of the assembly factor P-17 of bacteriophage PRD1,
- (iii) To study intramolecular disulfide bond containing cationic gemini surfactant and to observe the effects of its reductive cleavage in model membranes.

4. MATERIALS AND METHODS

4.1 MATERIALS

Except for F-DPPE (Molecular Probes), DHAB and DSP all lipids and GSH, calf thymus DNA, HEPES, and EDTA were from Sigma. DSP was synthesized as described in publication IV. For synthesis of DHAB see correction manuscript ¹⁰⁷ in the original publications section. Expression and purification of protein P17 was done as described previously ¹⁰⁸. Herring sperm DNA (average size of ≤ 2000 bp) was from Gibco BRL (Carlsbad, CA, USA) and sodium chloride from J. T. Baker (Deventer, Holland). The purity of lipids was checked by thin-layer chromatography on silicic acid coated plates (Merck, Darmstadt, Germany) using chloroform/methanol/water (65:25:4, by vol.) as a solvent system. Lipid concentrations were determined gravimetrically by using a high precision electrobalance (Cahn, Cerritos, CA, USA). DNA concentrations (in mM basepairs) were determined by absorbance at 260 nm ($\epsilon = 6600 \text{ cm}^{-1}\text{M}^{-1}$). Freshly deionized filtered water (Milli RO/Milli Q, Millipore Inc., Jaffrey, NH, USA) was used in all experiments.

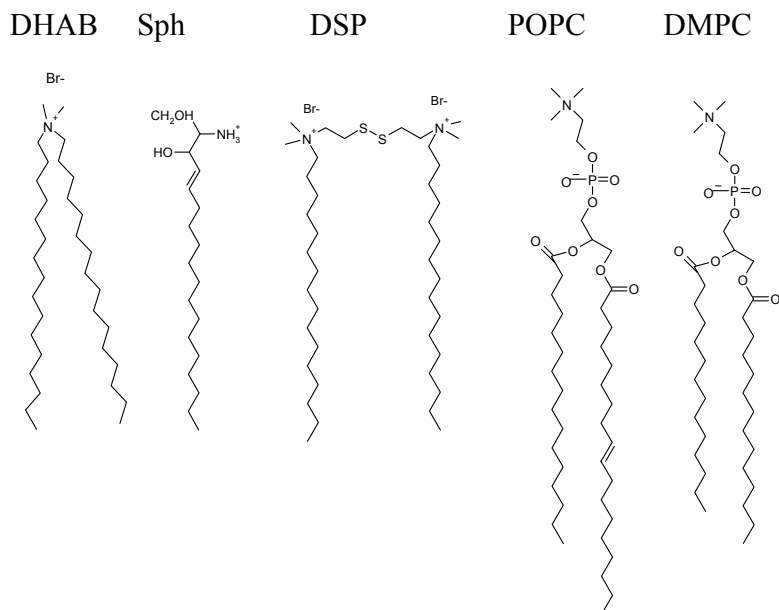


Figure 4.1. Chemical structures of the main amphiphiles used.

4.2 METHODS

4.2.1. Compression isotherms (I, II, IV)

A computer controlled Langmuir-type film balance μ ThrougS (I, II) or MicroThrough XS (IV), (Kibron Inc., Helsinki, Finland) was used to record compression isotherms (π -A). All glassware used was rinsed thoroughly with ethanol and purified water (Millipore). To ensure complete evaporation of the solvents the films were allowed to settle for 4 min before recording of π -A isotherms. Lipids were dissolved in chloroform and spread in this solvent onto the indicated aqueous phase at ≈ 25 °C. The monolayers were compressed at a rate of $4 \text{ \AA}^2/\text{molecule}/\text{min}$. Surface pressure π is defined as

$$\pi = \gamma_0 - \gamma$$

where γ_0 is the surface tension of the air/buffer interface and γ is the value for surface tension in the presence of a lipid monolayer compressed at varying packing densities. The reciprocal isothermal compressibility, i.e., the elastic modulus of area compressibility (C_S^{-1}) was calculated as described previously⁴⁵. Monolayer dipole potential ψ was measured using the vibrating plate method (μ Spot, Kibron Inc.).

4.2.2. Differential scanning calorimetry (III, IV)

Differential heat capacity scans were recorded using a high precision microcalorimeter (VP-DSC, MicroCal, Northampton, MA, USA). Prior to their loading into precooled DSC cuvettes, the samples were equilibrated on ice for at least 12 h. When indicated GSH was included to solution prior to incubation on ice (IV). The liposomes were scanned at a heating rate of 0.5 degrees per minute and data were collected during heating scans from 5 to 65 °C (III) or from 4 to 50 °C (IV). The instrument was interfaced to a PC, and the data were analyzed using the routines of the software provided by the instrument manufacturer.

4.2.3. Light scattering (III, IV)

Static light scattering due to liposome-P17 complex formation was measured with a Perkin-Elmer LS50B spectrofluorometer. The indicated LUV suspension was placed into a magnetically stirred four-window quartz cuvette thermostated at 30 °C. Scattering intensities were measured 3 min after the addition of P17 (III) at the indicated concentrations and were found to remain constant after this time period.

4.2.4 Resonance energy transfer (III)

The distance between appropriate fluorophore pairs can be assessed by Förster resonance energy transfer (RET). The association of R-P17 (rhodamine-P17) with membranes containing fluorescein-DPPE causes quenching of fluorescein emission while emission peak of rhodamine becomes observable, indicating resonance energy transfer between the dyes. Measurements were carried out with a Perkin-Elmer LS50B spectrofluorometer.

4.2.5. Detection of the cleavage of DSP on monolayers (IV)

Circular wells with Teflon rims and with gold plated bottom (subphase volume 6 ml, diameter 5 cm) were used for monitoring the changes in surface pressure π and surface dipole potential ψ after applying glutathione into the magnetically stirred subphase beneath the monolayer (IV). In some experiments herring sperm DNA (2.5 μ M) was included in the subphase prior to inclusion of glutathione.

4.2.6. Surface plasmon resonance (IV)

SPR measurements were performed with a Biacore 2000™ instrument using HPA sensor chips (Biacore AB, Uppsala, Sweden). The surface of the latter is composed of long-chain alkanethiol molecules forming a flat, quasi-crystalline hydrophobic layer. Coating of the HPA sensor surface with DSP was performed at +40°C following instructions of the manufacturer. In brief, the HPA chip surface was first washed for 5 min with 40 mM

n-octyl β -D-glucopyranoside and then coated with 1 mM DSP for 20 min, both at a flow rate of 5 μ l/min in water. Reduction of DSP on the HPA chip surface was performed with 3 mM glutathione. The binding of herring sperm DNA, 1 μ g/ml, was studied for DSP monolayer, after reduction of the surfactant and for uncoated HPA surface. The rate of flow in both measurements above was 5 μ l/min. Temperature was maintained at 25°C.

4.2.7. Determination of CMC (IV)

The CMC for DSP was determined at ambient temperature with a Delta-8 multichannel microtensiometer (Kibron Inc., Helsinki, Finland) and the isotherm analyzed with the Gibbs adsorption model embedded in the software (Delta-8 Manager) provided by the instrument manufacturer. For these measurements serial dilutions in the concentration range from 0.212 μ M to 1 mM in 150 mM NaCl were employed as indicated. To cleave DSP into its monomers 5 mM glutathione (final concentration) was added to 1 mM DSP solution and subsequently incubated at + 4 °C for 24 hours, prior to subjecting to serial dilution and assay for CMC.

4.5.8. Studies on giant vesicles (IV)

The indicated lipids were dissolved in diethylether : methanol (9:1, by vol.) to yield a final total lipid concentration of one mM. Four μ l of the above lipid solution was transferred on the surface of the two Pt electrodes in the GV formation chamber¹⁰⁹, and then dried under a gentle stream of nitrogen for at least 10 min¹¹⁰. A glass chamber with the attached electrodes and a quartz window bottom was placed on the stage of an inverted microscope (Olympus IX70, Olympus Optical co., Tokyo, Japan). An AC field was applied prior to adding the buffer. The AC field was turned off after 2-4 h, and GUVs were observed with differential interference contrast optics with a 10X/0.30 or 20X/0.40 objective. The sizes of the GUVs were measured using calibration of the images by motions of the micropipet as proper multiples of the step length (50 nm) of the micromanipulator (MX831 with MC2000 controller, SD Instruments, Grants Pass, OR).

When indicated small aliquots (approx. 50 picolitres) of glutathione (10 mM) corresponding to 0.5 picomoles of the reducing agent were applied from the micropipettes onto the outer surface of individual giant vesicles with a pneumatic microinjector (PLI-100, Medical Systems Corp., Greenvale, NY). All experiments were conducted with a Peltier-controlled thermal microscope stage (TS-4, Physitemp, Clifton, NJ, USA) set to 30 °C. Micropipets¹¹¹ with inner tip diameters of >0.5 µm were drawn from borosilicate capillaries (1.2 mm outer diameter) by a microprocessor-controlled horizontal puller (P-87, Sutter Instrument Co., Novato, CA).

5. RESULTS

5.1. MIXED MONOLAYERS OF POPC AND CATIONIC LIPIDS (I + II)

5.1.1. Characterization of mixed monolayers of POPC and DHAB: effects of DNA

Compression isotherms

The transfection efficiency of DHAB was enhanced by phosphatidylcholines and did not require the presence of helper lipid such as DOPE¹¹². Accordingly, we studied the mixed monolayers of DHAB and POPC in more detail and, moreover, used varying concentrations of DNA to observe whether it interacts with POPC/DHAB films. Similarly to POPC, DHAB formed stable monolayers at an air/water interface and its compression isotherms revealed a smooth π -A curve, lacking indications for structural transitions and indicating the film to be in the liquid expanded state (Fig. 5.1).

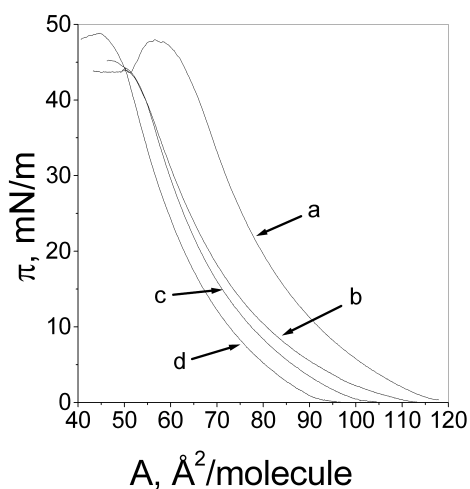


Figure 5.1. Representative π/A isotherms for (a) POPC, (b) DHAB, and their mixed monolayers recorded on a subphase of 5 mM HEPES, 0.1 mM EDTA, pH 7.4. The content of DHAB in the isotherms of the binary films shown was (c) $X_{\text{DHAB}} = 0.05$ and (d) $X_{\text{DHAB}} = 0.13$.

Compression isotherms for mixed POPC/DHAB monolayers at $X_{\text{DHAB}} < 0.5$ were smooth and revealed no discontinuities indicative of phase transitions. At $X_{\text{DHAB}} = 0.5$, however, a discontinuity in the π -A curve was evident at a surface pressure of 27 mN/m. This is more clearly present in π vs. elastic moduli C_S^{-1} plots (Fig. 5.4).

Analysis of the mean molecular areas revealed that already at $X_{\text{DHAB}} = 0.05$ the films were condensed and at 10 mN/m for instance a reduction by approx. 15 % was evident in the mean molecular area, from 92 to 78 \AA^2 (Fig. 5.2A). Maximal condensation was seen at $X_{\text{DHAB}} \approx 0.38$ after which the area/molecule increased with increasing X_{DHAB} and the monolayers slowly expanded back towards the isotherm of neat DHAB. The condensing effect of DHAB ($X_{\text{DHAB}} = 0.05$) on POPC monolayers did depend on the phosphocholine headgroup and was absent for the neutral dioleoylglycerol monolayers (I, Fig. 3).

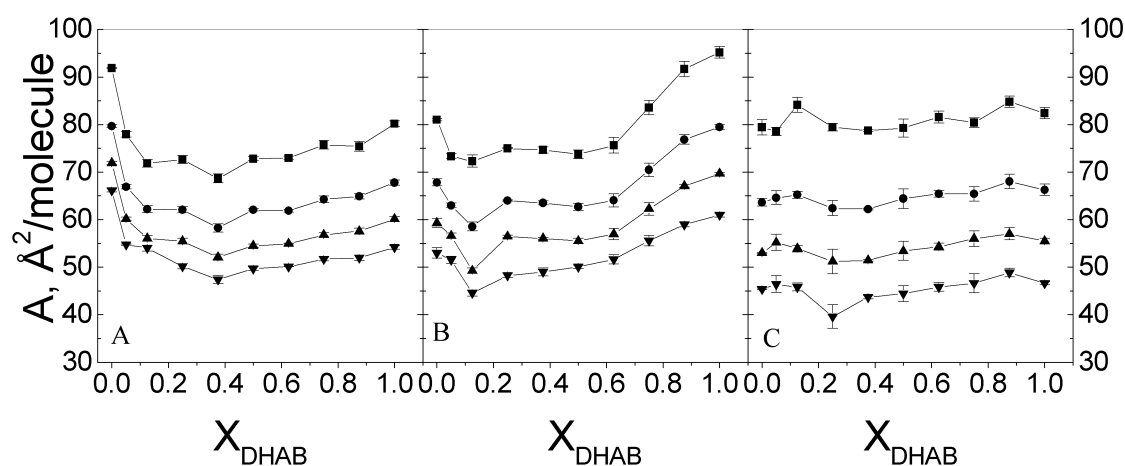


Figure 5.2. (Panel A). The effect of increasing X_{DHAB} on the area/molecule in compression isotherms of mixed POPC/DHAB films. The values of π were 10 (■), 20 (●), 30 (▲), and 40 mN/m (▼). (Panels B and C) Similar data recorded in the presence of 0.63 and 1.88 μM DNA (in basepairs) in the subphase, respectively.

Effects of DNA

Interestingly, including DNA into the subphase condensed neat POPC monolayers, for example at 10 mN/m from 92 to 80 $\text{\AA}^2/\text{molecule}$ (Fig. 5.2B). A condensing effect due to DNA was evident also in the presence of the cationic surfactant and did depend on the DNA/DHAB charge ratio. Accordingly, at 0.63 μM DNA film condensation remained up to $X_{\text{DHAB}} < 0.5$, corresponding to a DNA/DHAB charge ratio of approx. 2.5 (Fig 5.3). At $X_{\text{DHAB}} > 0.5$ an expansion was observed. When the concentration of DNA was increased to 1.88 μM basepairs, the films were condensed irrespective of X_{DHAB} (Fig 5.2C).

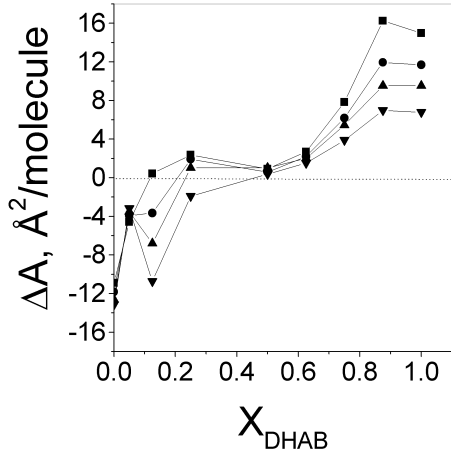


Figure 5.3. The difference in the area $A_{\text{DNA}}-A$ ($\text{\AA}^2/\text{molecule}$) as a function of X_{DHAB} . The values for A_{DNA} were recorded with $0.63 \mu\text{M}$ DNA (in basepairs) in the subphase and those for A without DNA. The values of π were 10 (\blacksquare), 20 (\bullet), 30 (\blacktriangle), and 40 mN/m (\blacktriangledown).

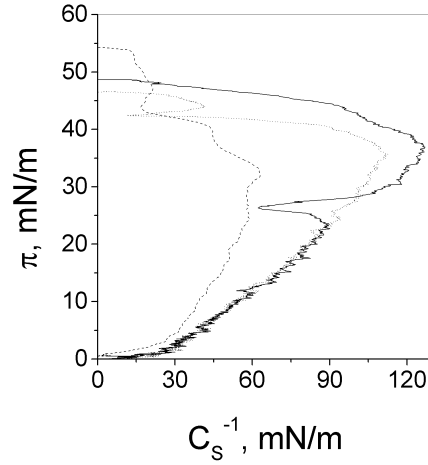


Figure 5.4. π vs. elastic moduli C_S^{-1} for monolayers at $X_{\text{DHAB}} = 0.5$ (solid line) and similar measurements but with either 0.63 (.....) or $1.88 \mu\text{M}$ (---) DNA (in basepairs) in the subphase.

Monolayer compressibility modulus

Representative π vs. C_S^{-1} data recorded at $X_{\text{DHAB}} = 0.5$ both without and with DNA in the subphase are illustrated in Fig. 5.4. In the absence of DNA the compressibility modulus C_S^{-1} decreased by $\approx 30\%$ at 27 mN/m , corresponding to the discontinuity in the π - A isotherm (I, Fig. 2). In the presence of $0.63 \mu\text{M}$ DNA the discontinuity in C_S^{-1} vs. A was evident at a pressure slightly above 40 mN/m , close to the collapse pressure of this monolayer. At higher DNA concentration resulting in DNA/DHAB charge ratio of 3.76 (at $X_{\text{DHAB}} = 1.0$) the values for C_S^{-1} were significantly reduced indicating an increase in the elasticity of the film.

Already low contents of DHAB ($X_{\text{DHAB}} = 0.05$) increased the maximum in compressibility modulus ($C_S^{-1}_{\text{max}}$) by approx. 30 and 20 mN/m in the absence and presence of $0.63 \mu\text{M}$ DNA, respectively (Fig. 5.5). Both with and without DNA the highest values were evident at $X_{\text{DHAB}} = 0.63$. Thereafter, with increasing X_{DHAB} the value of $C_S^{-1}_{\text{max}}$ diminished (i.e. the elasticity of the film increased) progressively. With higher concentrations of DNA in the subphase ($[\text{DNA}] = 1.88 \mu\text{M}$) the values for $C_S^{-1}_{\text{max}}$ were

significantly reduced and remained rather constant irrespective of X_{DHAB} . The elasticity minimum of the POPC film shifted to lower pressures when low contents of DHAB were included in the films, with the lowest value, ≈ 33 mN/m at $X_{\text{DHAB}} = 0.25$. When $0.63 \mu\text{M}$ DNA was included in the subphase the pressure yielding minimum in film elasticity decreased to 34 mN/m with neat POPC and decreased further to approx. 27 mN/m at $X_{\text{DHAB}} = 0.05$. Thereafter, a progressive increment to 37 mN/m at $X_{\text{DHAB}} = 0.63$ was observed. With higher concentration of DNA the values for $\pi_{C_s^{-1}\text{max}}$ were closer to those measured for lipids without DNA (Fig. 5.5.B).

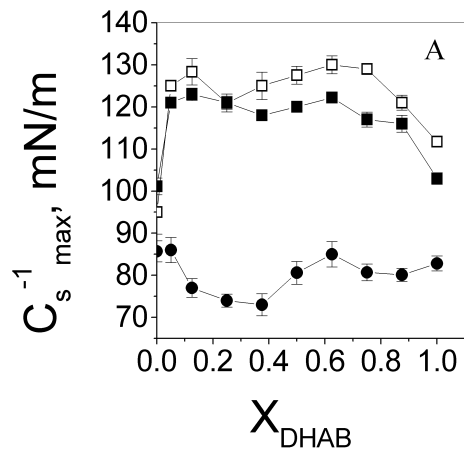
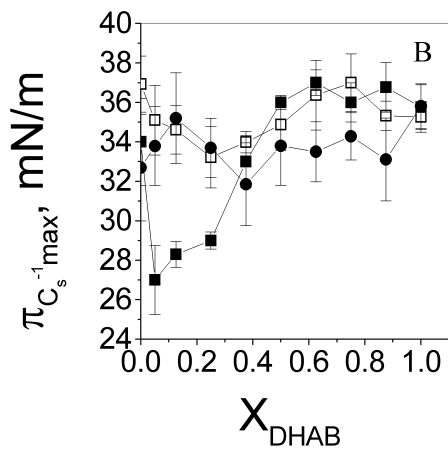


Figure 5.5. (Panel A). The dependence of C_s^{-1} on X_{DHAB} in mixed DHAB/POPC monolayers, recorded in the absence (\square) and in the presence of either 0.63 (\blacksquare) or 1.88 (\bullet) μM DNA (in basepairs).

(Panel B) Surface pressures π corresponding to the compressibility modulus maxima C_s^{-1} measured in the absence (\square), and in the presence either 0.63 (\blacksquare) or 1.88 (\bullet) μM DNA in the subphase.



In conclusion, the content of the cationic lipid in the monolayer strongly influenced both the mechanical and electrical properties of the film. A dramatic condensation was seen as a result of including low amounts of DHAB ($X_{\text{DHAB}} = 0.05$) in POPC monolayers evident as a decrease in area/molecule, reduced elasticity of the film, and increased monolayer dipole potential. Similarly to inclusion of DHAB, addition of DNA into the subphase resulted in condensation of POPC monolayers up to $X_{\text{DHAB}} = 0.5$. At $X_{\text{DHAB}} > 0.5$ an expansion due to DNA (0.63 μM in basepairs) was observed whereas in higher concentrations of DNA (1.88 μM in basepairs) the films remained condensed.

5.1.2. Sphingosine-phosphatidylcholine monolayers: effects of DNA

Force-area isotherms for sphingosine/POPC monolayers

Analysis of the mean molecular areas revealed that already at $X_{\text{Sph}} = 0.05$ the POPC films were condensed (by up to 30 % at a surface pressure $\pi = 35$ mN/m, Fig. 5.6A) similarly to what was observed for mixed films of the synthetic cationic surfactant DHAB and POPC. Upon exceeding $X_{\text{Sph}} = 0.05$ the films condensed further reaching a minimum at $X_{\text{Sph}} = 0.25$. Interestingly, after this first minimum the area/molecule increased significantly, with a relative expansion of the film towards the line representing ideal mixing and with a peak in A at $X_{\text{Sph}} = 0.38$. Upon exceeding $X_{\text{Sph}} = 0.38$ the area/molecule decreased again reaching a second minimum at $X_{\text{Sph}} = 0.63$. This minimum was followed by a sharp increase in A , reaching a second relative maximum at $X_{\text{Sph}} = 0.71$. Subsequently, increasing the molar content of sphingosine further to $X_{\text{Sph}} = 0.83$ revealed a third minimum in area/molecule where after $X_{\text{Sph}} = 1.0$ was reached without further discontinuities.

Effects of DNA

Binding of DNA to sphingosine containing cationic liposomes is well established^{19, 113} and its association with sphingosine containing films is anticipated. We repeated the above experiments with 2.5 μM DNA in the subphase to monitor the effects of this polyanion on POPC/sphingosine monolayers (Fig. 5.6B). The amount of DNA was chosen to yield complete saturation of the positive charges of sphingosine

(DNA/sphingosine charge ratio > 1 at $X_{\text{Sph}} = 1.0$). As mentioned previously, DNA condensed neat POPC monolayers, at 10 mN/m for example from 92 to 78 $\text{\AA}^2/\text{molecule}$. The shapes of the peaks in the area/molecule were changed and DNA condensed the films in the region of the peak at $X_{\text{Sph}} = 0.38$, as illustrated in the area difference ($\Delta A/\text{molecule}$) between isotherms measured in the presence and absence of 2.5 μM DNA (Fig. 5.6C).

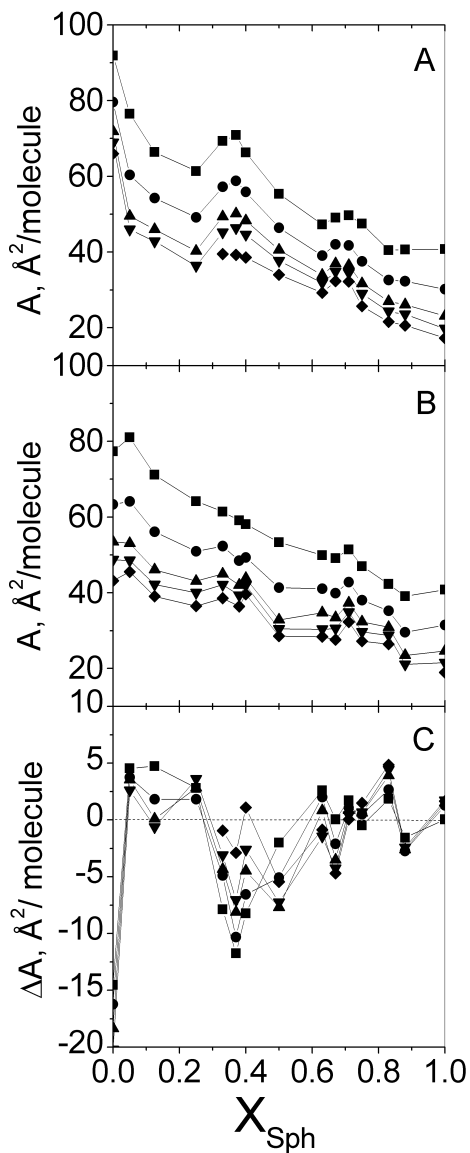


Figure 5.6. (A) The effect of increasing X_{Sph} on the area/molecule in compression isotherms of mixed POPC/Sph films. The values of π were 10 (\blacksquare), 20 (\bullet), 30 (\blacktriangle), 35 (\blacktriangledown), and 40 (\blacklozenge) mN/m. (B) Similar data recorded in the presence of 2.5 μM DNA (in basepairs) in the subphase, respectively. (C) The difference in the area $A_{\text{DNA}} - A$ ($\text{\AA}^2/\text{molecule}$) as a function of X_{Sph} .

The above data was expressed also in terms of the difference in the average area occupied by molecule between the measured values and ideal mixing of POPC and sphingosine in monolayers (Fig. 5.7). The steep initial decrease observed upon introducing sphingosine up to $X_{\text{Sph}} = 0.05$ was followed by a plateau in $\Delta A/\text{molecule}$ to $X_{\text{Sph}} = 0.25$ (Fig 5.7A). The range of $\Delta A/\text{molecule}$ changed drastically between $X_{\text{Sph}} = 0.25$ and $X_{\text{Sph}} = 0.38$. Upon exceeding $X_{\text{Sph}} = 0.38$ the $\Delta A/\text{molecule}$ decreased until after $X_{\text{Sph}} = 0.63$ a sharp increase was observed, revealing film expansion. The peak in area/molecule at $X_{\text{Sph}} = 0.71$ illustrated as $\Delta A/\text{molecule}$ also showed the films to be almost ideally mixed at higher surface pressures (from $\pi = 40$ to 30 mN/m) and close to ideal at lower pressures. With $2.5 \mu\text{M}$ DNA in the subphase the behavior of the films was somewhat different (Fig. 5.7B) but, however, discontinuities at approximately same molar proportions of sphingosine were evident both with and without DNA.

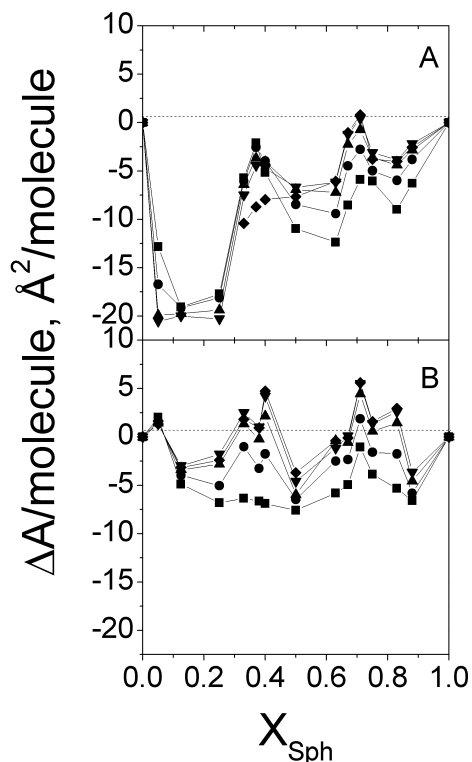


Figure 5.7. (A) The difference between measured values and ideal mixing $A_{\text{meas}} - A_{\text{ideal}}$ ($\text{\AA}^2/\text{molecule}$) as a function of X_{Sph} . (B) Similar data recorded in the presence of $2.5 \mu\text{M}$ DNA (in basepairs) in the subphase, respectively

Changes in monolayer dipole potential ψ

Taking into account the cationic charge of sphingosine containing monolayers and the interaction of polyanionic DNA with these films, alterations in the dipole potential⁴⁶ are readily anticipated. These data were recorded as a function of X_{Sph} and are depicted at varying molecular densities (Fig. 5.8).

The presence of sphingosine had a significant impact on the monolayer dipole potential and already at $X_{\text{Sph}} = 0.05$ a pronounced increment in Ψ was evident, at $2.5 \mu\text{mol}/\text{m}^2$ from 280 (neat POPC) to 380 mV. Between $X_{\text{Sph}} = 0.25$ and $X_{\text{Sph}} = 0.40$, however, a discontinuity in surface potential was observed, similarly to the area/molecule plots (Fig. 5.7A). Upon including a charge-saturating concentration of DNA into the subphase the monolayer dipole potential for POPC increased, at $2.5 \mu\text{mol}/\text{m}^2$ from approx. 280 to 330 mV, respectively (Fig. 5.8B). The presence of sphingosine further increased Ψ , up to 370 mV at $X_{\text{Sph}} = 0.05$ Ψ (at $2.5 \mu\text{mol}/\text{m}^2$). Upon increasing X_{Sph} from 0.25 to 0.5 a similar pattern of changes in dipole potential was observed when compared to the data recorded without DNA.

To better illustrate the impact of DNA these data are shown also as a function of X_{Sph} as the recorded voltage difference $\Delta\Psi$ for the monolayers with and without DNA in the subphase (Fig. 5.8C). An initial steep decrease until $X_{\text{Sph}} = 0.13$ was followed by an increase so that when increasing X_{Sph} from 0.25 to 1.0 the values of Ψ were slightly higher in the presence of DNA compared to its absence, with exceptions at $X_{\text{Sph}} = 0.5$, 0.67 and 0.71 where $\Delta\Psi$ was negative.

Excess free energy of mixing

Negative values of ΔG_m^{ex} for all the investigated composition ranges confirm that the mixing is energetically favorable and, accordingly, there should be no phase separation of the individual compounds (Fig. 5.9A). The minimum values, indicating the highest stability of the mixed phase, occurred in regions where the monolayer was the most condensed with respect to the ideal mixing (Fig. 5.7), from $X_{\text{Sph}} = 0.05$ to $X_{\text{Sph}} = 0.25$ and from $X_{\text{Sph}} = 0.5$ to $X_{\text{Sph}} = 0.63$ respectively. ΔG_m^{ex} was pressure dependent so that for

higher pressures the values of ΔG_m^{ex} decreased. This is expected as at higher packing densities the interactions between the molecules are stronger and also the differences derived from molecular characteristics for different compound molecules are larger. Upon increasing X_{Sph} the free energy became less negative indicating the interactions between the two components becoming weaker.

The presence of DNA altered the mixing energies dramatically (Fig. 5.9B and C). Accordingly, the values for ΔG_m^{ex} shifted from a highly negative values observed in the absence of DNA to close to zero, indicating the mixing of the components becoming less favorable. Notably, the most positive values were measured for the films at highest pressure. To better illustrate the effects of DNA to mixing properties of the components in the monolayer we calculated the difference between ΔG_m^{ex} measured both with and without DNA (Fig. 5.9C). With a charge saturating concentration of DNA in the subphase, the mixing of POPC and sphingosine became less favorable with the differences in ΔG_m^{ex} being largest at low X_{Sph} .

To conclude, even low contents of sphingosine ($X_{\text{Sph}} = 0.05$) condensed POPC monolayers similarly to what was observed with the synthetic cationic lipid DHAB (I). Intriguingly, the mixed films of POPC and sphingosine exhibited three critical mole fractions of sphingosine (0.25, 0.6, and 0.83) at which the area/molecule reached a local minimum. The observed minima were nearly completely absent when 200 mM NaCl was present in the aqueous subphase and also when POPC was replaced by either saturated or unsaturated diacylglycerol. According to excess free energy of mixing derived from the compression isotherms the mixed phase was most stable at the observed minima and upon increasing X_{Sph} the mixing of the two components became less favorable. Inclusion of a charge saturating concentration of DNA into the subphase led to a diminished monolayer stability and increased separation of the components.

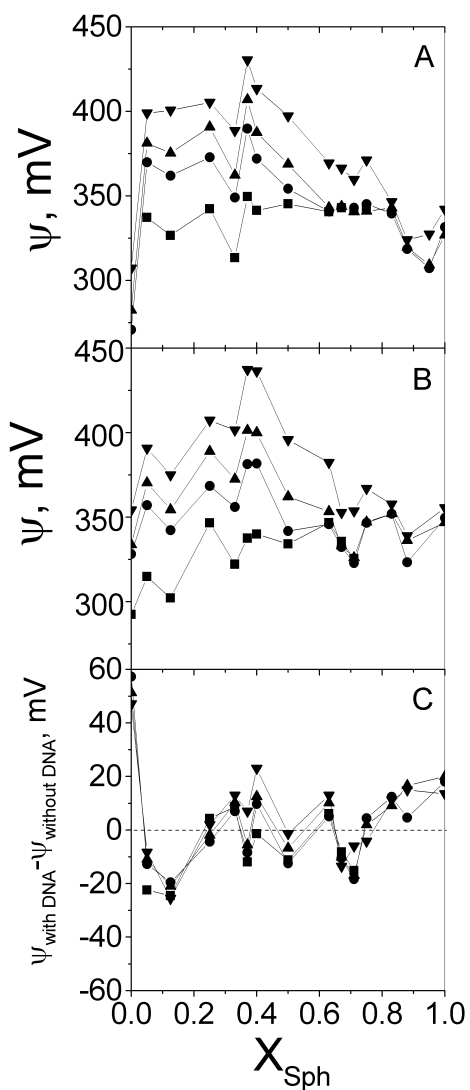


Figure 5.8. Values for monolayer dipole potential Ψ derived from compression isotherms for POPC/Sph monolayers as a function of X_{Sph} and recorded both without (A) and with 2.5 μM DNA (B) in the subphase. The data are shown at varying molecular densities, at 1.8 (\blacksquare), 2.3 (\bullet), 2.5 (\blacktriangle), and 2.9 (\blacktriangledown) $\mu\text{mol}/\text{m}^2$. Also shown is the voltage difference between the above data points, representing the impact of DNA on the monolayers (B).

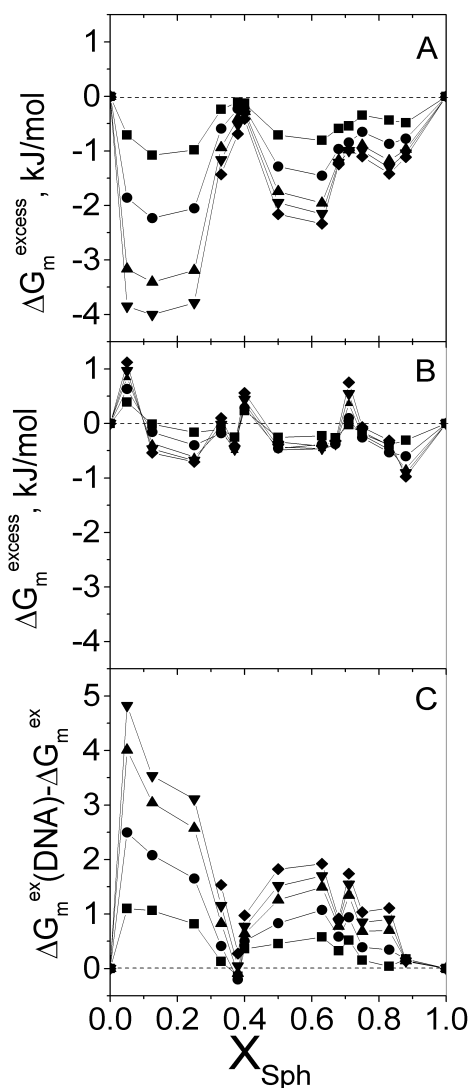


Figure 5.9. (A) Values for excess free energy of mixing derived from compression isotherms for POPC/Sph monolayers as a function of X_{Sph} . The values of π were 10 (\blacksquare), 20 (\bullet), 30 (\blacktriangle), 35 (\blacktriangledown), and 40 (\blacklozenge) mN/m . (B) Similar data recorded in the presence of 2.5 μM DNA (in basepairs) in the subphase, respectively. Also shown is the difference between the above data points, representing the impact of DNA on the monolayers (C).

5.2. LIPID PROTEIN INTERACTIONS (III)

The assembly factor P17 of a bacteriophage PRD1 possesses a net charge of -7 at pH 7.2. Previous studies suggest that P17 would act late in the phage assembly and thus possible interactions of P17 with membranes would be of importance.

Light scattering

In order to address this point we used light scattering (LS) to observe the interaction of P17 with LUVs. Three kinds of vesicles were used, namely those composed of only POPC, or additionally including negatively charged POPG (X = 0.10) or positively charged sphingosine (X = 0.10). For neat POPC LUVs increasing amounts of P17 in the samples caused a progressive increase in relative intensity (RI), with two stepwise increments (Fig. 5.10).

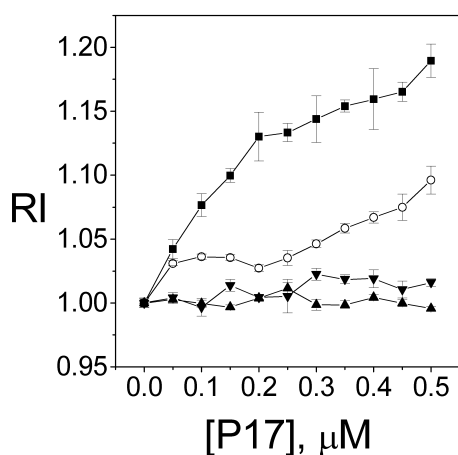


Figure 5.10. Relative intensity of scattered light at 90° due to the binding of P17 to liposomes composed of POPC (○), POPG/POPC (molar ratio 1:9, respectively) (▲), sphingosine/POPC (molar ratio 1:9, respectively) (■), and sphingosine/POPG/POPC (molar ratio 1:1:8, respectively) (▼). After the protein concentration was increased, the samples were equilibrated for 3 min before measuring the intensity. Total lipid concentration was $22.5 \mu\text{M}$ (at 30°C).

The addition of P17 up to $0.05 \mu\text{M}$ into neat POPC liposomes increased the scattering approximately 1.03-fold, while further addition of P17 (up to $0.2 \mu\text{M}$) had no additional effect. Exceeding a [P17] of $0.2 \mu\text{M}$ caused a continuous increase in RI with a maximum increment of approximately 1.1 fold observed at a [P17] of $0.5 \mu\text{M}$, corresponding to a phospholipid : P17 molar ratio of 45. The presence of the negatively charged POPG

($X_{\text{POPG}} = 0.10$) in the POPC LUVs totally abolished the increase in LS up to the highest concentration of P17 tested (0.5 μM). When the cationic sphingosine/POPC LUVs ($X_{\text{Sph}} = 0.10$) were used, the addition of P17 caused a significant increase in LS indicating association to sphingosine containing membranes. Moreover, the increase in LS could be prevented by adding 150 mM NaCl to the buffer or by including POPG into the vesicles.

Resonance energy transfer

We subsequently confirmed the association of P17 with liposomes using resonance energy transfer (RET) between fluorescein-DPPE (F-DPPE) incorporated into LUVs and rhodamine-P17 (R-P17). For POPG/POPC/F-DPPE LUVs (10:85:5) a negligible decrease in relative fluorescence intensity (RFI) was observed upon addition of R-P17 up to 0.45 μM (Fig. 5.11). For POPC/F-DPPE LUVs (95:5) a more pronounced decrease in RFI was evident at R-P17 concentrations higher than 0.15 μM . However, the most efficient energy transfer was observed for sphingosine/POPC/F-DPPE LUVs (10:85:5), with a 31 % decrease in the emission of F-DPPE at a [R-P17] of 0.45 μM .

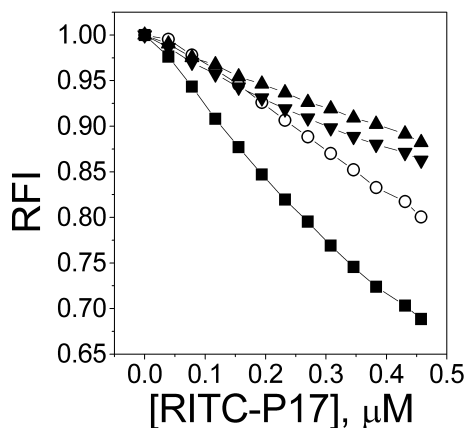


Figure 5.11. Binding of P17 to liposomes as revealed by resonance energy transfer. Relative fluorescence intensity at different concentrations R-P17 upon binding to liposomes composed of POPC/F-DPPE (95:5) (○), POPG/POPC/F-DPPE (10:85:5) (▲), sphingosine/POPC/F-DPPE (10:85:5) (■), and sphingosine/POPG/POPC/F-DPPE (10:10:75:5)(▼).

Time course of the binding

We then proceeded to study the kinetics of this interaction between P17 and lipid membranes. As shown in Fig. 5.12, the rapid decrease (approximately 4%) in RFI after the addition of R-P17 (0.25 μ M; lipid-to-protein ratio 90:1) to POPG/POPC/F-DPPE LUVs (10:85:5) was caused by non-specific effects such as scattering, dilution, and inner filter effects. After this, there was practically no further decrease in RFI for these liposomes. However, when POPC/F-DPPE LUVs (95:5) were used together with 0.25 μ M R-P17 in the samples, the rapid initial decrease was approximately 8% higher than that observed for LUVs containing POPG. Thereafter a small time dependent decrease in RFI was observed.

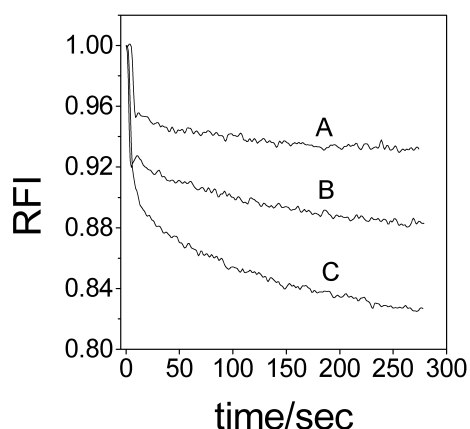


Figure 5.12. Time course of the binding of R-P17 to liposomes. In trace A liposomes were POPG/POPC/F-DPPE (10:85:5), in trace B POPC/F-DPPE (95:5), and in the lowest trace (trace C) sphingosine/POPC/F-DPPE (10:85:5).

When using sphingosine/POPC/F-DPPE LUVs (10:85:5) a clear time dependent decrease in RFI is observed upon incubation with 0.25 μ M P17. After an initial decrease in RFI (approximately 10 %), a further slow decrease could be observed, reaching saturation after approximately 250 s.

Differential scanning calorimetry

Neat DMPC MLVs showed a pretransition at approximately 14 $^{\circ}$ C and a main transition at 23.9 $^{\circ}$ C (Fig. 5.13A). The incorporation of P17 into DMPC MLVs (phospholipid : P17,

47:1) did change only slightly the main transition temperature. However, there was a significant increase in the enthalpy of the transition (ΔH) by about 3.8 kJ/mol. The width of the peak, inversely proportional to the co-operativity of the phase transition, was insignificantly affected. DMPG : DMPC (1:9) showed a slightly increased phase transition temperature, ΔH , and peak width compared to neat DMPC MLVs (Fig. 5.13B). Including P17 into these liposomes resulted in a small decrease in T_m , with a concomitant small increase (approximately 1 kJ/mol) in ΔH . Sphingosine : DMPC MLVs (1:9) displayed a single transition peak centered at 26.4 °C (Fig. 5.13C) with ΔH increasing by approximately 2.7 kJ/mol compared to that observed for neat DMPC. Moreover, the co-operativity of the transition decreased upon incorporation of sphingosine, as evidenced by the increased width of the main transition peak. The addition of P17 into sphingosine-containing MLVs induced dramatic changes in the heating scan. As shown in Fig. 5.13, panel C, the pretransition disappeared and the main transition temperature T_m shifted 2.4 °C higher with two clearly distinct peaks becoming evident. ΔH increased 0.7 kJ/mol with the peak being approximately 3.7 °C wider than in the absence of P-17.

To summarize, our data showed that P17 binds to positively charged membranes containing sphingosine whereas only weak binding was evident to neutral POPC vesicles, and no binding at all for the negatively charged vesicles containing POPG. DSC data suggested that P17 induces lipid phase separation and tighter packing in sphingosine : DMPC vesicles and that for membranes lacking the positive charge addition of P17 has virtually no effect.

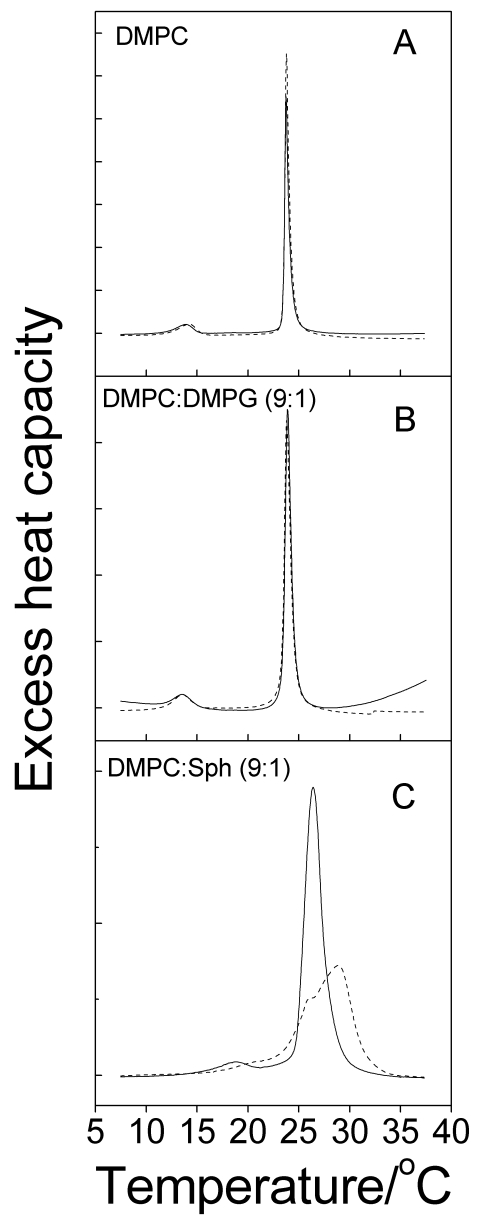


Figure 5.13. Apparent excess heat capacity traces of lipid vesicles in buffer with and without P17. **Panel A**, DMPC MLVs (solid trace) alone and with P17 (dashed trace). **Panel B**, DMPG/DMPC MLVs (1:9) alone (solid trace) and in the presence of P17 (dashed trace). **Panel C**, sphingosine/DMPC MLVs (1:9) as such (solid trace) and with P17 (dashed trace). [P17] was 15 μM .

5.3. REDUCTIVE CLEAVAGE OF DISULFIDE BOND CONTAINING CATIONIC GEMINI SURFACTANT IN MONOLAYERS AND IN BILAYERS (IV)

The chains of a gemini surfactant DSP are linked via a disulfide bond containing spacer and thus this surfactant can be cleaved by reduction into two monomers (MSP), representing conventional cationic surfactants.

CMC

The CMC for the gemini surfactant DSP (see Fig. 4.1 for structure) in 150 mM NaCl was $7.5 \pm 0.3 \mu\text{M}$, in keeping with the low values reported for geminis⁷⁹ when compared to conventional surfactants. For MSP the CMC was $12.1 \pm 0.8 \mu\text{M}$ (Fig. 5.14).

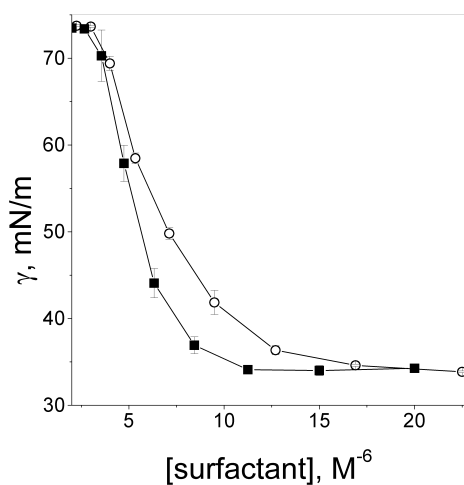


Figure 5.14. Surface tension vs. concentration for DSP (solid squares) and MSP (open circles) in 150 mM NaCl. Temperature was $\approx 24^\circ\text{C}$.

When reducing [NaCl] in the buffer the CMC for MSP increased and in pure deionized water it was 20 fold higher whereas for DSP the increase was only $2.5 \mu\text{M}$ (7.5 vs. $10 \mu\text{M}$).

Differential scanning calorimetry

Upon heating DSP exhibited a main endotherm with a peak at 21.7 °C with a total enthalpy of ~84.4 kJ/mol (Fig. 5.15, line a). Reduction of DSP with 5 mM GSH caused pronounced changes in the endotherm, decreasing the peak temperature to 20.1 °C and reducing the enthalpy content to 68.54 kJ/mol. The endotherm also became significantly broader thus indicating less co-operative melting (Fig. 5.15, line b).

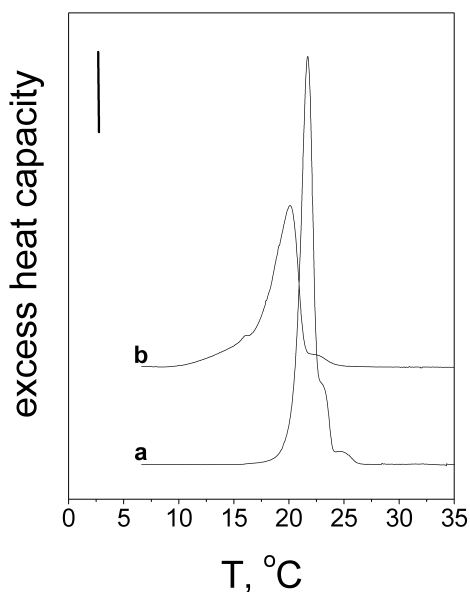


Figure 5.15. DSC traces for one mM DSP in 150 mM NaCl as such (a) and after incubation for 24 hours with 5 mM GSH (b). The calibration bar represents 10 kJ°C⁻¹mol⁻¹.

Monolayer experiments

DSP formed stable monolayers when 150 mM NaCl was present in the subphase. The compression isotherms for DSP were smooth with C_S^{-1} further supporting the lack of phase transitions. To monitor the reductive cleavage of DSP in monolayers we injected GSH into the magnetically stirred subphase, while recording changes in π and Ψ . The addition of GSH caused a decrease both in π as well as in Ψ (Fig. 5.16A) with a new equilibrium reached in ~30 min, and with an average decrement of 9.7 mN/m (\pm 3.3 mN/m). Simultaneously, the value for Ψ decreased by approx. 32.9 mV (\pm 15.9 mV). These experiments were reproduced using a range of initial surface pressure values (varying from 10.9 to 18.6 mN/m) yielding surface dipole potentials from 99.9 to 161.1 mV, respectively.

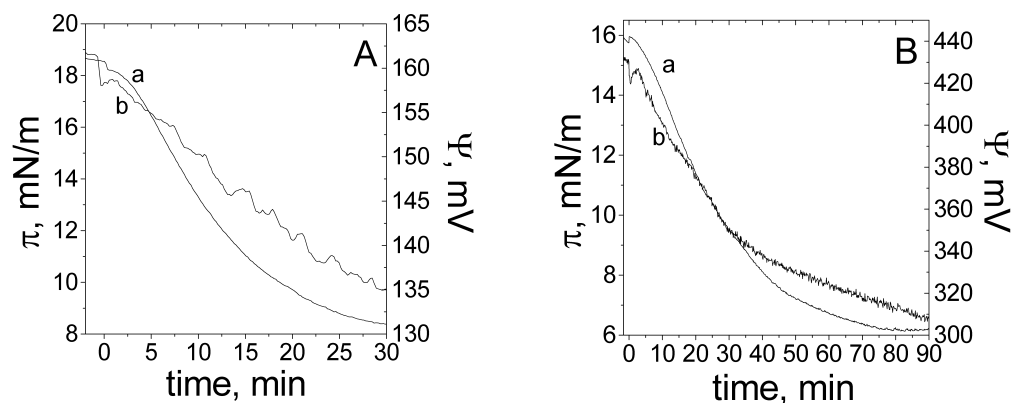


Figure 5.16. (A) Changes in surface pressure π (a) and surface dipole potential Ψ (b) as a function of time following the addition GSH, [final]=55 μ M, into the subphase of 150 mM NaCl. (B) Similar experiment but recorded in the presence of 2.5 μ M DNA (in base pairs) in the subphase.

The values for Ψ increased dramatically when DNA present (Fig. 5.16B), at 16 mN/m, for example, from \sim 155 mV to \sim 420 mV, yielding a difference of 0.15 fV/molec.. Moreover, following the addition of GSH it took approx. three to four times longer (30 min vs. 90-120 min) for the monolayers to reach a new equilibrium in the presence of DNA than in its absence.

Surface Plasmon Resonance experiments

Supported monolayers of DSP were studied using surface plasmon resonance (SPR). Decrement in the response from approximately 250 to 80 (RU) was evident when the monolayers were flushed with 3 mM GSH (Fig. 5.17A), in keeping with the release of DSP. Similarly to Langmuir monolayers a new steady state was reached in \sim 30 min. GSH induced a minor increment in the response level for the uncoated chip, presumably resulting from non-specific binding of the peptide to the gold surface. The attachment of DNA to the supported DSP monolayer and the impact of reductive cleavage by GSH was also studied (Figure 5.17B). DNA readily bound to DSP monolayers, as expected, whereas no binding was evident to the GSH treated DSP membranes or to the uncoated chips.

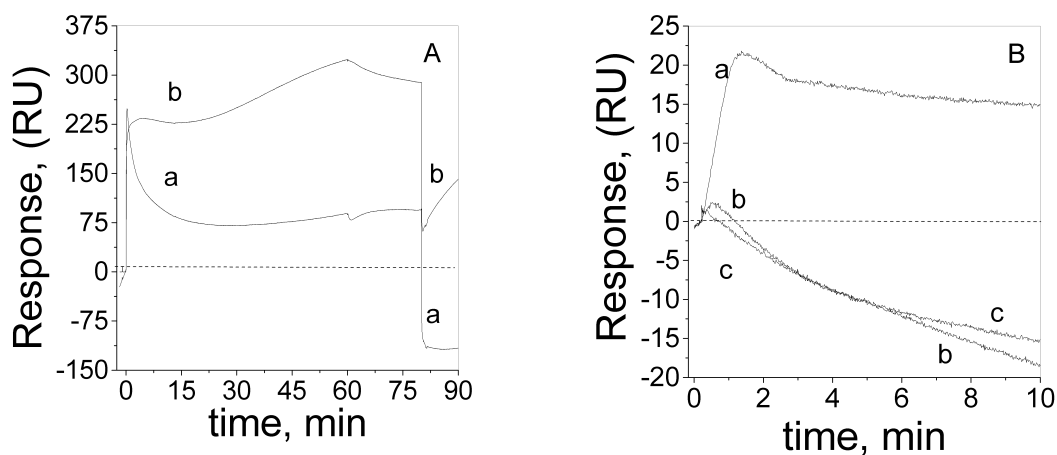


Figure 5.17. (A) SPR response following the addition of 3 mM GSH into the aqueous phase rinsing the supported DSP monolayer on the sensor chip surface (a), with uncoated HPA surface as a control (b). (B) Binding of DNA (1 $\mu\text{g/ml}$) to a DSP monolayer (a) after the reduction of the surfactant with glutathione (b). Uncoated HPA surface (c) was used as a control.

Studies with GUVs and LUVs.

The size of GUVs formed by SOPC and DSP ($X_{\text{DSP}} = 0.10$) varied between approx. 20–100 μM . GSH (10 mM) was injected with gentle pressure using a micropipette onto the surface of a single GUV. Interestingly, in several experiments a bright spot came visible within approx. 5 seconds after the addition of GSH, moving on the GUV surface. In about 20 seconds the spot pinched off from the GUV surface and the GUV started shrinking. This process continued at an accelerating rate and led to the disappearance of the GUV in ~ 30 seconds (Fig. 5.18). In control experiments the same amount of the buffer (0.5 mM HEPES, pH 7.4) injected in a similar manner produced no changes in GUV morphology. Addition of GSH did not have any significant effect on SOPC/DSP ($X_{\text{DSP}} = 0.10$) LUVs, monitored by static light scattering.

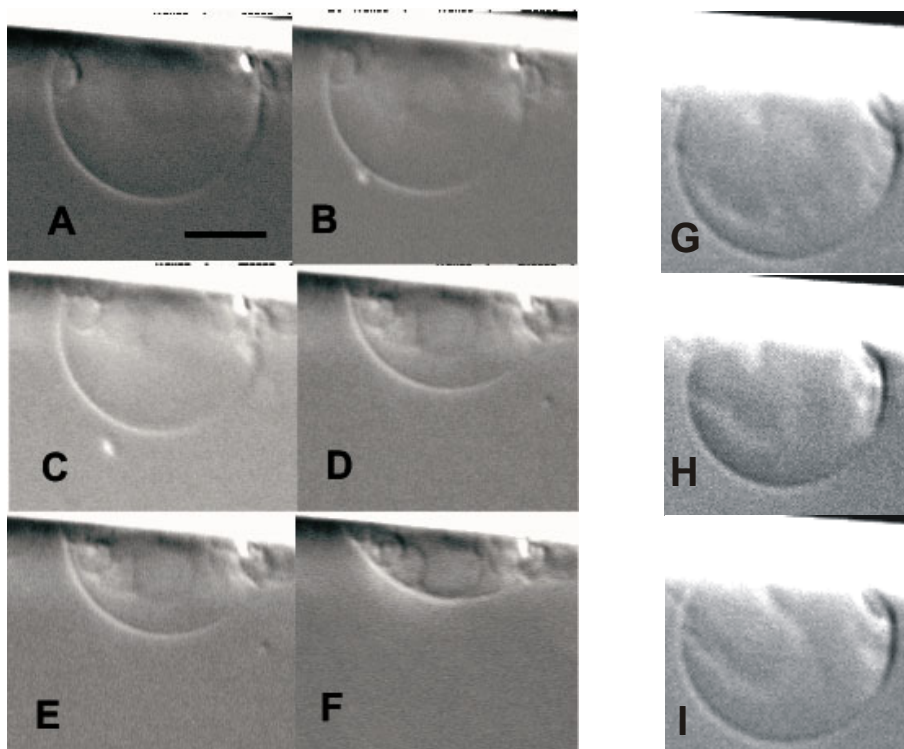


Figure 5.18. Changes in the morphology of a GUV (SOPC:DSP, 9:1 molar ratio) recorded before (A) and (B) 5, (C) 10, (D) 15, (E) 20, and (F) 30 sec after the addition of approx. 50 picoliter aliquot of 10 mM glutathione (corresponding to ~ 0.5 picomoles of GSH) onto the GUV surface with a micropipette. Temperature was 30°C . Scale bar = $20\ \mu\text{m}$.

Panels G – I represent a control experiment where buffer (0.5 mM HEPES, pH 7.4) was injected in a similar manner.

In conclusion, the intramolecular disulfide bridge containing gemini surfactant DSP was readily cleavable by glutathione in monolayers as well as in vesicles. In 150 mM NaCl CMC for DSP was $7.5\ \mu\text{M}$ whereas that of the monomer MSP was $12.1\ \mu\text{M}$. The endotherm for the MSP was significantly broader indicating less co-operative melting. For Langmuir films of DSP the addition of GSH into the subphase led to a decrease in surface pressure π as well as surface dipole potential Ψ . The presence of a charge saturating concentration of DNA significantly attenuated the cleavage, but it did not prevent the reaction. The resulting monomers detached from supported monolayers, leading to loss of affinity of the surface for DNA. Disruption of giant vesicles containing DSP within approx. 30 s following a local injection of GSH was observed, revealing membrane destabilization.

6. DISCUSSION

Eukaryotic cells are literally packed with lipid membranes and the different membranous organelles with unique lipid compositions perform different functions²⁹. Any single membrane can contain over 100 lipid species and the lipid distribution in various membranes is non-uniform and carefully regulated. The enormous diversity of the membrane lipids points out to their multiple roles in determining the properties and interactions of membranes. Charged lipids are of special interest, since they have been established to control important physiological functions and as minor membrane components their quantities are under strict metabolic control⁶². The interaction of these charged lipids with biological macromolecules is a product of complex hydrophobic, electrostatic, and steric constraints and, as such, essential for the functioning of a living cell.

6.1. MIXING FAR FROM IDEAL: monolayers of POPC and DHAB(I) or SPH(II)

In the following section mixed monolayers of zwitterionic POPC and either synthetic DHAB (I) or naturally occurring cationic lipid sphingosine (II) are discussed. In the original publication I a stoichiometric mixture of a monocationic surfactant DHAB and *N,N*-dimethyl-3,4-dimethylpyrrolidinium bromide was used instead of the desired dicationic gemini surfactant due to reasons described in the erratum (see original publications). *N,N*-dimethyl-3,4-dimethylpyrrolidinium bromide as a water soluble compound, however, did not influence the monolayer behavior of the mixed DHAB/POPC films and thus our conclusions concerning the role of the surface charge density in the organization of monolayers remain valid. The combined molecular weight of the mixture is the same as for the gemini surfactant and, accordingly, the concentrations and the mole fractions of the lipids are correct. The correct DNA/CL charge ratios are, however, twice the values given due to DHAB bearing a single positive charge instead of two used in the calculations for the gemini. The corrected structure and nomenclature described in erratum is used throughout this thesis.

6.1.1 Reorientation of the phosphocholine dipole

Introducing positively charged DHAB into POPC monolayers induced significant condensation of the films. Already low amounts of the cationic lipid ($X_{\text{DHAB}} = 0.05$) caused a condensation of 15 % at 10 mN/m, for example. The condensation was absent when DHAB was added into monolayers composed of either saturated or unsaturated diacylglycerol (I, Fig. 3). The maximum in condensation was observed at $X_{\text{DHAB}} = 0.38$ after which the monolayer slowly expanded, in keeping with molecular dynamics simulation on DMPC/DMTAP bilayers¹¹⁴. Similar condensation with respect to the ideal mixing was recently reported also for mixtures of cationic surfactant DODAB and zwitterionic DSPC¹¹⁵. The negative deviation from the ideal mixing throughout the range of molar fractions of DHAB from 0.05 to 0.875 can be considered surprising since by introducing cationic lipids into the membrane increases the surface charge density. This, in turn, should lead to increased coulombic repulsion between lipids of same charge and thus expand the monolayer. A plausible explanation for the observed behavior derives from the zwitterionic nature of the PC headgroup. Choline moiety is known to be able to orient in the direction of the membranes normal and as, in contrast to PE, the hydrophobic methyl group in the headgroup does not form hydrogen bonds with water the orientation of the PC headgroup is susceptible to changes¹¹⁶. Upon introducing one positive charge with each DHAB to the membrane the dipole of the PC headgroup could turn to a more vertical orientation, so as to maximize the distance between the positive charges of DHAB and the choline moiety. After exceeding $X_{\text{DHAB}} = 0.38$ the increasing coulombic repulsion leads to film expansion towards neat DHAB monolayers. Recent DSC and fluorescence data on DHAB/DMPC vesicles show augmented packing again in higher charge densities ($X_{\text{DHAB}} > 0.6$) and as an explanation the formation of an interdigitated phase is suggested¹¹⁷. In monolayers the interdigitation is, of course, not an option and thus the monolayer can not escape from expansion. The above mechanisms for condensing effect of the cationic DHAB or sphingosine would cause augmented chain-chain interactions in keeping with the pronounced reduction in the interfacial elasticity of the film (Fig. 5.5) as well as increase in T_M observed in DSC (Fig. 5.13.). A

schematic illustration showing the reorientation of the P⁻-N⁺ dipole is presented in Fig. 6.1. The impact of DNA is discussed later in this thesis.

The reorientation of the PC headgroup has been observed with several methods: by monolayers for DMPC¹¹⁸, by DSC for DMPC and DPPC^{94, 119}, by molecular modeling for DMPC¹²⁰, and by NMR for POPC¹¹³. However, thorough characterizations of mixed cationic lipid – phosphatidylcholine – films were lacking before our studies.

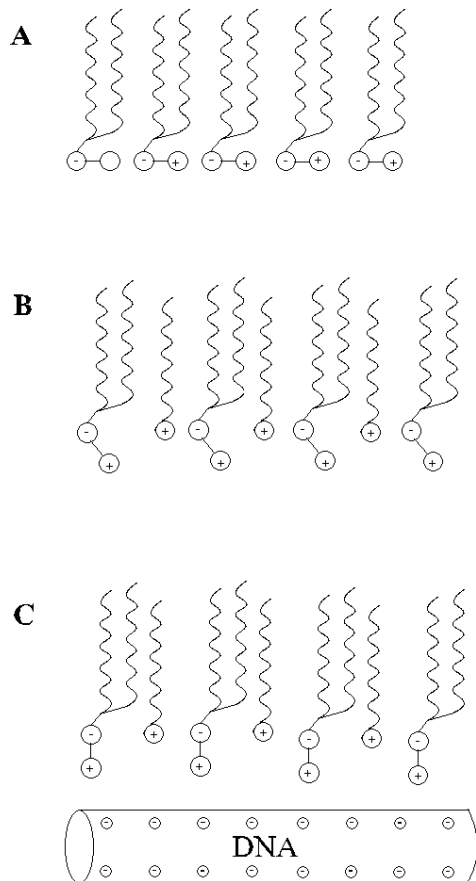


Figure 6.1. A schematic illustration of the reorientation of the P⁻-N⁺ dipole induced by cationic lipid and DNA (Modified from Ryhänen et al. 2003).

6.1.2. A highly sensitive mole fraction dependent mixing

Similarly to what observed with DHAB the pronounced condensation of the POPC films following the introduction of the cationic lipid was evident already at low concentrations of sphingosine ($X_{\text{Sph}} = 0.05$). This effect is likely to be of electrostatic origin since it was absent for diacylglycerol and, in addition, sphingosine ($X_{\text{Sph}} = 0.05$) induced dramatic increase in monolayer dipole potential in POPC monolayers (Fig. 5.8).

Mixed monolayers of POPC and sphingosine exhibited three critical mole fraction dependent condensation minima, viz., $X_{\text{Sph}} = 0.25$, 0.6, and 0.83. The following mechanisms could allow for the observed counterintuitive behavior of the mixed sphingosine and POPC monolayers: (i) reorientation of the phosphocholine dipoles, (ii) condensation of counterions with their release increasing entropy, (iii) formation of hydrogen bonded networks, and (iv) lateral diffusion and reorganization of the components in the monolayer.

Reorientation of the $\text{P}^- \text{-N}^+$ dipole of POPC is likely to take place when sphingosine is included and this should contribute to the observed monolayer condensation. As described above in chapter 6.1.1. the reorientation is well documented in other systems and with several methods. At first, increasing the content of sphingosine would lead to more complete reorientation of the dipole observed as decreased surface areas. Exceeding certain charge density in the monolayer ($X_{\text{DHAB}} = 0.38$ in DHAB/POPC monolayers, for example) then leads to increased coulombic repulsion and thus also expansion of the monolayer.

In addition to the former process, the counterions in the surrounding media also affect the membrane. As concluded by Cevc¹²¹ the membrane surfaces are too complex for any of the available electrostatic theories to be reliable for their general description and thus explaining the observed phenomena is likely to require combinations of different models and interactions. In Gouy-Chapman electrostatic theory the ion distribution close to the membrane surface is governed by the coulombic surface–ion interactions. Importantly,

the ion concentration near the membrane surface differs from the bulk over a zone of finite thickness. Changes in the monolayer composition can lead to changes in the layer of counterions so that both their condensation and release from the membrane surface are possible¹²². Dissociation of counterions from the surface would lead to changes in the entropy of the system that may contribute to the observed behavior.

Hydrogen bonding needs to be considered as well. We may assume miscibility of POPC and sphingosine based on the negative values of ΔG_m^{ex} (Fig. 5.9). Interestingly, ΔG_m^{ex} reveals a shift towards less negative values with increasing X_{Sph} observed after every local minimum in the area/molecule. The interactions between POPC and sphingosine are enhanced at higher surface pressures, $\Delta G_m^{\text{ex}} \sim -4.0$ kJ/mol at $X_{\text{Sph}} = 0.13$ and at $\pi = 35$ mN/m, compared to ~ -1.0 kJ/mol at $\pi = 10$ mN/m, for example (Fig. 5.9A) meaning that in keeping with this at higher molecular densities the energetic benefits gained by efficient packing are more significant. To reduce free energy increase caused by increased positive surface charge density upon increasing X_{Sph} , the extent of protonation of the NH_2 moiety should decrease. It is possible, that the protonated and deprotonated forms of sphingosine associate via hydrogen bonding and that their lateral segregation could lead to different ordering depending on the membrane composition similarly to that suggested for acidic phospholipids^{90, 123}.

Lastly, it is possible that monolayer components could associate in a regular lattice¹²⁴. To illustrate this, we calculated if the lipid stoichiometries corresponding to the critical mole fractions ($X_{\text{Sph}} = 0.25, 0.6,$ and 0.83) would allow for regular lateral patterns of lipid distribution, maximizing the distance between sphingosine and thus minimizing their mutual coulombic repulsion. One possible way of ordering sphingosine and POPC is represented in Fig. 6.2. At $X_{\text{Sph}} = 0.25$ a superlattice can be assembled consisting of a unit cell with one acyl chain of sphingosine being surrounded by six acyl chains of POPC (i.e., three POPC molecules), yielding the maximal distance between the positively charged sphingosines. The presented superlattice should be considered to take place as a time averaged ordering only.

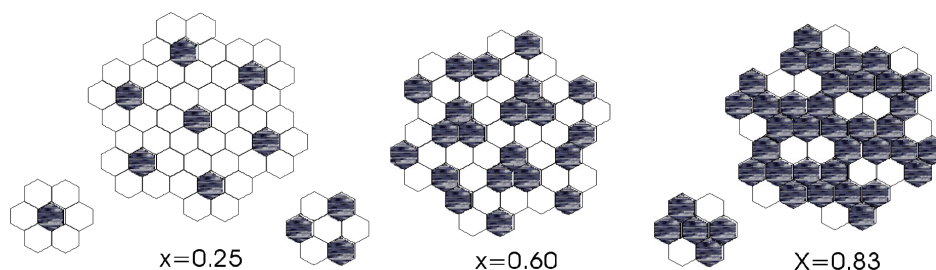


Figure 6.2. Putative mean lateral arrangements of acyl chains in Sph/POPC monolayers with corresponding unit cells. White and gray hexagons represent the acyl chains of POPC and the alkyl chain of sphingosine, respectively.

Charged membranes are surprisingly complex structures and attempts to combine the exact mechanisms, interactions, and forces responsible for the observed several condensation minima are challenging. The above mechanisms can, at least to some extent, take place at the same time and it is the balance between all the forces together that matters.

6.1.3. Surface dipole potential

Phospholipid headgroups have been shown to be sensitive to electric charges and dipole fields¹¹⁶ and structural, dielectric and spectroscopic measurements indicate that the P^+-N^- dipole orients almost in parallel to the plane of the membrane surface in the pure phospholipid membrane. As discussed above, introducing a cationic amphiphile into the POPC monolayer results in efficient condensation of the film indicating reorientation of the PC dipole. In keeping with the above we observed a significant increase in Ψ upon introducing cationic lipid into POPC monolayer (I and II). Already at $X_{DHAB} = 0.05$ there was an increase of 100 mV in Ψ at 127 pmol/cm^2 and an increase of similar magnitude was evident also with sphingosine (Fig. 5.8). Further increasing the amount of cationic lipid led to a steep increase in Ψ up to $X_{DHAB} = 0.25$ after which a smaller, yet significant, steady increase was observed. Estimates from NMR studies indicate that the change in the orientation of the phosphate segment can be more than 30° ¹¹³ and it is likely that

maximal average angle is reached at high molar fractions of the cationic amphiphile. The total increase in Ψ at 127 pmol/cm^2 and at $X_{\text{Sph}} = 0.5$ was approx. 180 mV. This would be large enough to trigger conformational changes in the membrane proteins or to facilitate protein insertion into membranes, for example, and thus also probably bears biological significance^{46, 125}. Even though charged lipids are minor components in biological membranes our results indicate that their effects on membrane dipole potential and thus to the interplay between the cell surface and its surroundings can be crucial.

6.2. THE INTERACTIONS OF MEMBRANES AND CHARGED MACROMOLECULES

The main interactions in a cell should include protein – protein, protein – nucleic acid, lipid – lipid, lipid – protein, and lipid – nucleic acid interactions. Especially the latter remain poorly resolved but, owing to recent interest in liposomal gene delivery, these interactions have begun to raise considerable attention. We used model membranes to characterize the complex interplay between lipids and charged macromolecules, namely DNA (I, II, IV) and protein (III).

6.2.1. Interaction of DNA with charged monolayers

Similarly to addition of small amounts of cationic lipid ($X_{CL} = 0.05$) to POPC monolayers inclusion of DNA into the subphase resulted in significant condensation (Figs. 5.3 and 5.6). This is likely to result from DNA associating weakly to the monolayer causing the P⁻-N⁺ dipole to reorient vertically, as explained for the condensing effect of CL. Interestingly, the effect of DNA to the monolayer turns into expanding at $X_{DHAB} > 0.5$ (exceeding DNA/DHAB charge ratio of two). This could arise from DNA inducing local demixing of the monolayer components^{83, 100} in keeping with the observations from X-ray studies⁸⁹. Lateral heterogeneity in the lipid distribution would then result in film expansion due to persistence length of DNA¹²⁶. Increased attraction of DNA towards monolayers with higher density of positive charges is likely to contribute to the expansion as well. In line with the above is the diminished monolayer stability in the presence of DNA observed in POPC/SPH monolayers (Fig. 5.9B and C). The mixing of sphingosine and POPC is less favorable in the presence of DNA as ΔG_m^{ex} changes from highly negative (in the absence of DNA) to even positive at certain values of X_{SPH} . Accordingly, the free energy of binding for DNA overcomes the free energy loss caused by local reorganization of the compounds. The driving force for this effect might be the more complete release of counterions from DNA and the film, allowed by local charge densities. In addition to the above changes also monolayer dipole potential changed when a charge-saturating concentration of DNA was included in the subphase. For neat POPC

monolayer, for example, there was an increase of approximately 50 mV (from 280 to 330 mV) at $2.5 \mu\text{mol}/\text{m}^2$ (Fig. 5.8). Interestingly, in transfection experiments enhanced efficiency was evident at $X_{\text{DHAB}} \geq 0.5$ underlining the surface electrostatics being a crucial player in lipofection⁹⁴.

6.2.2. The interaction of protein P17 with positively charged lipid membranes

The mode of action of the bacteriophage assembly factor P17 has remained elusive. Previous studies suggested that the protein would act in the formation of the viral particle itself¹⁰⁸ and interactions of this assembly factor with the emerging membrane are possible. Electrostatic interactions commonly mediate the binding of peripheral proteins to charged lipid surfaces^{11, 102}. As these interactions certainly play an important role in regulation of cellular functions it was reasonable to undertake a study of the possible direct interactions of protein P17 with model membranes.

P17 carries a net negative charge of -7 at pH 7.2 and it is thus likely that it interacts with positively charged membranes as well as with other proteins. Light scattering, resonance energy transfer and differential scanning calorimetry revealed strong interactions of positively charged sphingosine containing membranes and P17. Accordingly, the initial binding of P17 involves electrostatically driven interactions possibly mediated by the presence of lipid microdomains. In keeping with the electrostatics being the key player only weak binding was evident with neutral lipid membranes. Membrane association of P17 could be reversed by POPG, a negatively charged amphiphile, thus neutralizing the charges. Moreover, the increase in LS could be prevented by adding 150 mM NaCl to the buffer. Sphingosine ($X_{\text{Sph}} = 0.10$) induced an increase in T_m of approx. 2.7 °C for DPPC MLVs in keeping with the condensing effect observed in monolayer studies (I, II). To this end, the addition of cationic sphingosine into zwitterionic DPPC vesicles is likely to cause reorientation of the P⁻-N⁺ dipole of the PC headgroup which is expected to result in reduced repulsive interactions at the headgroup level. As a result chain-chain interactions are augmented evident as elevated values for T_m .

6.3. REDUCTIVE CLEAVAGE OF A GEMINI SURFACTANT: IMPLICATIONS FOR GENE DELIVERY

In order to overcome the poor release of DNA from lipoplexes and to diminish the cytotoxicity of cationic vectors reducible cationic lipids have been designed^{80, 127-130}. The intramolecular disulfide bridge containing lipids are expected to release DNA upon reduction by intracellular glutathione. Aligned with this approach also reducible cationic gemini surfactants have been synthesized⁸⁰.

The disulfide bridge of gemini surfactant DSP (see Fig. 4.1. for structure) was readily cleaved by glutathione (GSH) in free standing monolayers on an air-water interface, in supported monolayers on solid surfaces, and in giant vesicles. CMC for DSP in water was very low, 10 μM , as expected for a gemini surfactant, while that for the monomer MSP was ~ 0.22 mM. In keeping with the increased surface tension of water and augmented screening of the surfactant charges the CMCs decreased progressively in the presence of increasing NaCl concentrations. More specifically, for the gemini surfactant the stronger hydrophobicity due to two interconnected acyl chains leads to lower CMCs compared to single-chained monomer MSP irrespective to [counterion]. For MSP the inclusion of counterions has a more dramatic effect as the reduced coulombic repulsion helps to overcome the energetic barriers that keep the monomer free in the solution and thus inhibit the packing of MSP into micelles or interfaces. Accordingly, in 130 mM NaCl the CMCs for DSP and MSP were 8.4 and 36 μM , and in 150 mM NaCl 7.5 and 12.1 μM respectively.

Inclusion of GSH into the subphase of DSP monolayer on air-water interface, or to the water-flow on supported monolayer, resulted in escape of lipid from the surface. Aligned with the above CMCs, reductive cleavage of DSP is likely to result in MSP monomers partitioning to subphase. This was evident as decrease of both π and Ψ as well as response (RU) in surface plasmon resonance (SPR) with roughly similar kinetics (Figs. 5.16 and 5.17). In giant vesicles, the microinjection of GSH onto the surface resulted in shrinkage of the GUV in ca. 30 s. Interestingly, in several experiments a bright spot

appeared on the GUV surface within approx. 5 s. after the addition of GSH and the spot pinched off from the surface in about 20 seconds. It is possible that the spot contains clustered monomers and that some of the lipid also escape from the GUV in the form of micelles. In LUVs no changes following the addition of GSH were observed, indicating the membrane curvature playing a crucial role in the membrane perturbation. For an individual gemini surfactant in a giant vesicle the membrane is almost planar and the packing will be closer to that in monolayer than in LUVs.

The practical value of the type of chemical reduction described above has been claimed to be limited by inefficient cleavage in the presence of DNA¹³¹. To this end the reduction of DSP was evident also in the presence of DNA even though the kinetics of the chemical cleavage was significantly slower than in its absence (30 vs. 90 min). Steric hindrance by DNA bound to the headgroup of DSP would readily explain this attenuation but, importantly, the presence of DNA did not inhibit the process. Moreover, our SPR experiments provided evidence for diminished affinity of the MSP monomers for DNA further suggesting that this gemini could be suitable for transfection *in vivo*.

7. ACKNOWLEDGEMENTS

These studies were carried out in the Department of Medical Chemistry (currently Biochemistry), Institute of Biomedicine at the University of Helsinki during years 1999-2005. I thank Professors Olli Jänne, Ismo Virtanen, and Esa Korpi for putting the facilities at my disposal.

It has been a privilege to work under the inspiring guidance of Professor Paavo Kinnunen. I wish to thank you for sharing your enormous experience in biophysics and everlasting enthusiasm towards science in general. Paavo has created a group, HBBG, where the creative and ease atmosphere has made the work a great pleasure. During these years the people in HBBG have become friends and I wish to thank all of You *Juha-Matti Alakoskela, Shambunath Bose, Christian Code, Yegor Domanov, Ove Eriksson, Morten Hagen, Juha Holopainen, Arimatti Jutila, Zhu Keng, Paola Luciani, Juha-Pekka Mattila, Antti Metso, Irina Moilanen, Kaija Niva, Antti Pakkanen, Mikko Parry, Tommi Paukku, Oula Peñate Medina, Tuula Peñate Medina, Jussi Pirneskoski, Samppa Ryhänen, Karen Sabatini, Rohit Sood, Kristiina Söderholm, Tim Söderlund, Kaija Tiilikka, Esa Tuominen, Ilkka Tuunainen, and Zhao Hong Xia* for all the nice time. I would especially want to thank the co-authors of the original publications of this thesis. Special thanks to Juha-Matti for patiently explaining everything I did not understand and also for letting me use your library. I appreciate your knowledge. Mikko has helped me with various computer-related problems, thank you for everything. Thank you, Samppa, for being my closest collaborator these six years, in disappointments as well as moments of success.

The reviewers of this thesis, docent Peter Mattjus, Åbo Akademi University, and docent Gerhard Gröbner, University of Umeå, are acknowledged for most helpful comments and constructive criticism.

I wish to thank Kaima, Mikko and Jani, my best friends from the early years in Kemijärvi, for all the things we have gone through. My warmest thanks go also to friends

and colleagues in Cursus Unicus, Spexi and in Curvatura –so long and thanks for all the skiing.

Finally I would like to express my deepest gratitude to my parents Marja-Leena and Erkki for everlasting support and love. I wish also to thank my brother Jussi and his family, Katja, Silja and Aarni for their friendship.

Most of all, thank you, Leena, for sharing your life with me.

This study was financially supported by the Research Foundation of Orion Corporation, the Finnish Cultural Foundation, Emil Aaltonen Foundation, Finnish Medical Society Duodecim, and Finnish Medical Foundation.

Helsinki, December 2005

Matti Säily

8. REFERENCES

- (1) Rose, H. G.; Frenster, J. H. *Biochim. Biophys. Acta* **1965**, *106*, 577-591.
- (2) Kinnunen, P. K. J.; Rytömaa, M.; Köiv, A.; Lehtonen, J.; Mustonen, P.; Aro, A. *Chem. Phys. Lipids* **1993**, *66*, 75-85.
- (3) Köiv, A.; Palvimo, J.; Kinnunen, P. K. J. *Biochemistry (N. Y.)* **1995**, *34*, 8018-8027.
- (4) Tigyi, G.; Goetzl, E. J.; Editors **2002**, 322.
- (5) Din, J. N.; Newby, D. E.; Flapan, A. D. *BMJ [British Medical Journal]* **2004**, *328*, 30-35.
- (6) Horrobin, D. F. *Prostaglandins, Leukotrienes and Essential Fatty Acids* **1999**, *60*, 431-437.
- (7) Crawford, M. A.; Bloom, M.; Broadhurst, C. L.; Schmidt, W. F.; Cunnane, S. C.; Galli, C.; Gehbremeskel, K.; Linseisen, F.; Lloyd-Smith, J.; Parkington, J. *Lipids* **1999**, *34*, S39-S47.
- (8) Singer, S. J.; Nicolson, G. L. *Science (Washington, DC, United States)* **1972**, *175*, 720-731.
- (9) Mouritsen, O. G. In *Life - as a matter of fat The Emerging Science of Lipidomics*; Dragoman, D., Dragoman, M., Elitzur, A. C., Silverman, M. P., Tuszynski, J. and Zeh, H. D., Eds.; The Frontiers Collection; Springer: Germany, 2005; Vol. 1, pp 275.
- (10) Cantor, R. S. *J Phys Chem B* **1997**, *101*, 1723-1725.
- (11) Heimburg, T.; Angerstein, B.; Marsh, D. *Biophys. J.* **1999**, *76*, 2575-2586.
- (12) Kinnunen, P. K. J. *Cellular Physiology and Biochemistry* **2000**, *10*, 243-250.
- (13) Jensen, M. O.; Mouritsen, O. G. *Biochim. Biophys. Acta* **2004**, *1666*, 205-226.
- (14) Felgner, P. L.; Gadek, T. R.; Holm, M.; Roman, R.; Chan, H. W.; Wenz, M.; Northrop, J. P.; Ringold, G. M.; Danielsen, M. *Proc. Natl. Acad. Sci. U. S. A.* **1987**, *84*, 7413-7417.
- (15) Lasic, D. D., Ed.; In *Liposomes In Gene Delivery*. CRC Press. Boca Raton, FL; 1997; .

- (16) Weichselbaum, R. R.; Kufe, D. *Lancet* **1997**, *349*, 10-12.
- (17) Hacein-Bey-Abina, S.; Le Deist, F.; Carlier, F.; Bouneaud, C.; Hue, C.; De Villartay, J. P.; Thrasher, A. J.; Wulffraat, N.; Sorensen, R.; Dupuis-Girod, S.; Fischer, A.; Davies, E. G.; Kuis, W.; Leiva, L.; Cavazzana-Calvo, M. *N. Engl. J. Med.* **2002**, *346*, 1185-1193.
- (18) Hacein-Bey-Abina, S.; Von Kalle, C.; Schmidt, M.; McCormack, M. P.; Wulffraat, N.; Leboulch, P.; Lim, A.; Osborne, C. S.; Pawliuk, R.; Morillon, E.; Sorensen, R.; Forster, A.; Fraser, P.; Cohen, J. I.; de Saint Basile, G.; Alexander, I.; Wintergerst, U.; Frebourg, T.; Aurias, A.; Stoppa-Lyonnet, D.; Romana, S.; Radford-Weiss, I.; Gross, F.; Valensi, F.; Delabesse, E.; Macintyre, E.; Sigaux, F.; Soulier, J.; Leiva, L. E.; Wissler, M.; Prinz, C.; Rabbitts, T. H.; Le Deist, F.; Fischer, A.; Cavazzana-Calvo, M. *Science* **2003**, *302*, 415-419.
- (19) Kõiv, A.; Kinnunen, P. K. *J. Chem. Phys. Lipids* **1994**, *72*, 77-86.
- (20) Kinnunen, P. K. *Chem. Phys. Lipids* **1991**, *57*, 375-399.
- (21) Nelson, D. L.; Cox, M. M. In *Lehninger Principles of Biochemistry*; Geller, E., Ed.; Lehninger Principles of Biochemistry; Worth Publishers: NY, USA, 2000; Vol. III, pp 1152-1.
- (22) Hilgemann, D. W. *Annu. Rev. Physiol.* **2003**, *65*, 697-700.
- (23) Gorter, E.; Grendel, F. *J. Exp. Med.* **1925**, *41*, 439-443.
- (24) Israelachvili, J. N. *Biochim. Biophys. Acta* **1977**, *469*, 221-225.
- (25) Sackmann, E. *Handbook of Biological Physics* **1995**, *1A*, 1-63.
- (26) Thompson, T. E.; Tillack, T. W. *Annu. Rev. Biophys. Biophys. Chem.* **1985**, *14*, 361-386.
- (27) Goodsaid-Zalduondo, F.; Rintoul, D. A.; Carlson, J. C.; Hansel, W. *Proc. Natl. Acad. Sci. U. S. A.* **1982**, *79*, 4332-4336.
- (28) Simons, K.; Ikonen, E. *Nature (London)* **1997**, *387*, 569-572.
- (29) Gennis, R. B. In *Biomembranes -Molecular structure and function*; Cantor, C. R., Ed.; Springer Advanced Texts in Chemistry; Springer: New York, 1989; Vol. 1, pp 533.
- (30) Alberts, B.; Johnson, A.; Lewis, J.; Raff, M.; Roberts, K.; Walter, P.; Editors **2002**, 1463.
- (31) Kinnunen, P. K. *J. Handbook of Nonmedical Applications of Liposomes* **1996**, *1*, 153-171.

- (32) Israelachvili, J. N.; Marcelja, S.; Horn, R. G. *Q. Rev. Biophys.* **1980**, *13*, 121-200.
- (33) de Vries, A. H.; Yefimov, S.; Mark, A. E.; Marrink, S. J. *Proc. Natl. Acad. Sci. U. S. A.* **2005**, *102*, 5392-5396.
- (34) Evans, E.; Kwok, R. *Biochemistry (N. Y.)* **1982**, *21*, 4874-4879.
- (35) Needham, D.; Evans, E. *Biochemistry (N. Y.)* **1988**, *27*, 8261-8269.
- (36) Needham, D.; McIntosh, T. J.; Evans, E. *Biochemistry (N. Y.)* **1988**, *27*, 4668-4673.
- (37) Marsh, D. *Biochim. Biophys. Acta* **1996**, *1286*, 183-223.
- (38) Cantor, R. S. *Biochemistry (N. Y.)* **1997**, *36*, 2339-2344.
- (39) Patra, M. *Los Alamos National Laboratory, Preprint Archive, Condensed Matter* **2005**, 1-10, arXiv:cond-mat/0504101.
- (40) Franklin, B. *Phil. Trans. R. Soc* **1774**, *64*, 445--.
- (41) Pockels, A. *Nature* **1891**, *43*, 437--.
- (42) Langmuir, I. *J. Am. Chem. Soc.* **1917**, *39*, 1848-1906.
- (43) Blodgett, K. B. *J. Am. Chem. Soc.* **1935**, *57*, 1007-1022.
- (44) Brockman, H. *Curr. Opin. Struct. Biol.* **1999**, *9*, 438-443.
- (45) Smaby, J. M.; Kulkarni, V. S.; Momsen, M.; Brown, R. E. *Biophys. J.* **1996**, *70*, 868-877.
- (46) Brockman, H. *Chem. Phys. Lipids* **1994**, *73*, 57-79.
- (47) Brezesinski, G.; Möhwald, H. *Adv. Colloid Interface Sci.* **2003**, *100-102*, 563-584.
- (48) Als-Nielsen, J.; Jacquemain, D.; Kjaer, K.; Leveiller, F.; Lahav, M.; Leiserowitz, L. *Physics Reports* **1994**, *246*, 251-313.
- (49) Kaganer, V. M.; Möhwald, H.; Dutta, P. *Rev. Mod. Phys.* **1999**, *71*, 779-819.
- (50) Weis, R. M. *Chem. Phys. Lipids* **1991**, *57*, 227-239.
- (51) Holopainen, J. M.; Brockman, H. L.; Brown, R. E.; Kinnunen, P. K. J. *Biophys. J.* **2001**, *80*, 765-775.
- (52) Daniels, C. B.; Orgeig, S. *Comparative Biochemistry and Physiology, Part A: Molecular & Integrative Physiology* **2001**, *129A*, 9-36.
- (53) Goerke, J. *Biochim. Biophys. Acta* **1998**, *1408*, 79-89.

- (54) Veldhuizen, R.; Nag, K.; Orgeig, S.; Possmayer, F. *Biochim. Biophys. Acta* **1998**, *1408*, 90-108.
- (55) Bangham, A. D.; Standish, M. M.; Watkins, J. C. *J. Mol. Biol.* **1965**, *13*, 238-252.
- (56) Luisi, P. L.; Walde, P.; Editors **2000**, 408.
- (57) Menger, F. M.; Angelova, M. I. *Acc. Chem. Res.* **1998**, *31*, 789-797.
- (58) Holopainen, J. M.; Angelova, M. I.; Söderlund, T.; Kinnunen, P. K. *J. Biophys. J.* **2002**, *83*, 932-943.
- (59) Nurminen, T. A.; Holopainen, J. M.; Zhao, H.; Kinnunen, P. K. *J. Am. Chem. Soc.* **2002**, *124*, 12129-12134.
- (60) Walde, P. In *Enzymatic Reactions in giant Vesicles*; Luisi, Pier Luigi and Walde, Peter, Ed.; Giant Vesicles Perspectives in Supramolecular Chemistry Volume 6; Wiley: Zurich, Switzerland, 2000; pp 297-311.
- (61) Angelova, M. I.; Tsoneva, I. *Chem. Phys. Lipids* **1999**, *101*, 123-137.
- (62) Langner, M.; Kubica, K. *Chem. Phys. Lipids* **1999**, *101*, 3-35.
- (63) Zhang, L.; Granick, S. *Proc. Natl. Acad. Sci. U. S. A.* **2005**.
- (64) Cravatt, B. F.; Prospero-Garcia, O.; Siuzdak, G.; Gilula, N. B.; Henriksen, S. J.; Boger, D. L.; Lerner, R. A. *Science (Washington, D.C.)* **1995**, *268*, 1506-1509.
- (65) De Petrocellis, L.; Melck, D.; Bisogno, T.; Di Marzo, V. *Chem. Phys. Lipids* **2000**, *108*, 191-209.
- (66) Walker, J. M.; Krey, J. F.; Chu, C. J.; Huang, S. M. *Chem. Phys. Lipids* **2002**, *121*, 159-172.
- (67) Lees, G.; Dougalis, A. *Brain Res.* **2004**, *997*, 1-14.
- (68) Hannun, Y. A.; Loomis, C. R.; Merrill, A. H., Jr.; Bell, R. M. *J. Biol. Chem.* **1986**, *261*, 12604-12609.
- (69) Merrill, A. H., Jr.; Stevens, V. L. *Biochim. Biophys. Acta* **1989**, *1010*, 131-139.
- (70) Olivera, A.; Rivera, J. *Journal of Immunology* **2005**, *174*, 1153-1158.
- (71) Alewijnse, A. E.; Peters, S. L. M.; Michel, M. C. *Br. J. Pharmacol.* **2004**, *143*, 666-684.
- (72) Friedrichs, G. S.; Swillo, R. E.; Jow, B.; Bridal, T.; Numann, R.; Warner, L. M.; Killar, L. M.; Sidek, K. *J. Cardiovasc. Pharmacol.* **2002**, *39*, 18-28.

- (73) Igarashi, Y.; Hakomori, S.; Toyokuni, T.; Dean, B.; Fujita, S.; Sugimoto, M.; Ogawa, T.; El-Ghendy, K.; Racker, E. *Biochemistry (N. Y.)* **1989**, *28*, 6796-6800.
- (74) McDonald, O. B.; Hannun, Y. A.; Reynolds, C. H.; Sahyoun, N. *J. Biol. Chem.* **1991**, *266*, 21773-21776.
- (75) Colombaioni, L.; Garcia-Gil, M. *Brain Res. Rev.* **2004**, *46*, 328-355.
- (76) Mustonen, P.; Lehtonen, J.; Kõiv, A.; Kinnunen, P. K. J. *Biochemistry (N. Y.)* **1993**, *32*, 5373-5380.
- (77) Kõiv, A.; Mustonen, P.; Kinnunen, P. K. J. *Chem. Phys. Lipids* **1993**, *66*, 123-134.
- (78) Kirby, A. J.; Camilleri, P.; Engberts, J. B. F. N.; Feiters, M. C.; Nolte, R. J. M.; Soderman, O.; Bergsma, M.; Bell, P. C.; Fielden, M. L.; Garcia Rodriguez, C. L.; Guedat, P.; Kremer, A.; McGregor, C.; Perrin, C.; Ronsin, G.; van Eijk, M. C. P. *Angewandte Chemie, International Edition* **2003**, *42*, 1448-1457.
- (79) Menger, F. M.; Keiper, J. S. *Angewandte Chemie, International Edition* **2000**, *39*, 1907-1920.
- (80) Wetzer, B.; Byk, G.; Frederic, M.; Airiau, M.; Blanche, F.; Pitard, B.; Scherman, D. *Biochem. J.* **2001**, *356*, 747-756.
- (81) Ryhänen, S. J.; Säily, V. Matti J.; Parry, M. J.; Luciani, P.; Mancini, G.; Kinnunen, P. K. J.
- (82) Säily, V. Matti J.; Ryhänen, S. J.; Jutila, A.; Parry, M. J.; Kinnunen, Paavo K. J. *Cell. Mol. Biol. Lett.* **2005**, *10*, 43--.
- (83) Kõiv, A.; Mustonen, P.; Kinnunen, P. K. J. *Chem. Phys. Lipids* **1994**, *70*, 1-10.
- (84) Kennedy, M. T.; Pozharski, E. V.; Rakhmanova, V. A.; MacDonald, R. C. *Biophys. J.* **2000**, *78*, 1620-1633.
- (85) Ijiro, K.; Shimomura, M.; Tanaka, M.; Nakamura, H.; Hasebe, K. *Thin Solid Films* **1996**, *284-285*, 780-783.
- (86) Okahata, Y.; Kobayashi, T.; Tanaka, K. *Langmuir* **1996**, *12*, 1326-1330.
- (87) Bhaumik, A.; Ramakanth, M.; Brar, L. K.; Raychaudhuri, A. K.; Rondelez, F.; Chatterji, D. *Langmuir* **2004**, *20*, 5891-5896.
- (88) Chen, X.; Wang, J.; Shen, N.; Luo, Y.; Li, L.; Liu, M.; Thomas, R. K. *Langmuir* **2002**, *18*, 6222-6228.
- (89) Symietz, C.; Schneider, M.; Brezesinski, G.; Moehwald, H. *Macromolecules* **2004**, *37*, 3865-3873.

- (90) Subramanian, M.; Jutila, A.; Kinnunen, P. K. J. *Biochemistry (N. Y.)* **1998**, *37*, 1394-1402.
- (91) Alesci, S.; Ramsey, W. J.; Bornstein, S. R.; Chrousos, G. P.; Hornsby, P. J.; Benveniste, S.; Trimarchi, F.; Ehrhart-Bornstein, M. *Proc. Natl. Acad. Sci. U. S. A.* **2002**, *99*, 7484-7489.
- (92) Felgner, P. L.; Ringold, G. M. *Nature* **1989**, *337*, 387-388.
- (93) Wheeler, C. J.; Sukhu, L.; Yang, G.; Tsai, Y.; Bustamente, C.; Felgner, P.; Norman, J.; Manthorpe, M. *Biochim. Biophys. Acta* **1996**, *1280*, 1-11.
- (94) Ryhänen, S. J.; Säily, M. J.; Paukku, T.; Borocci, S.; Mancini, G.; Holopainen, J. M.; Kinnunen, P. K. J. *Biophys. J.* **2003**, *84*, 578-587.
- (95) Huebner, S.; Battersby, B. J.; Grimm, R.; Cevc, G. *Biophys. J.* **1999**, *76*, 3158-3166.
- (96) Sternberg, B.; Sorgi, F. L.; Huang, L. *FEBS Lett.* **1994**, *356*, 361-366.
- (97) Paukku, T.; Lauraeus, S.; Huhtaniemi, I.; Kinnunen, P. K. J. *Chem. Phys. Lipids* **1997**, *87*, 23-29.
- (98) Pedroso de Lima, M. C.; Neves, S.; Filipe, A.; Duzgunes, N.; Simoes, S. *Curr. Med. Chem.* **2003**, *10*, 1221-1231.
- (99) Simberg, D.; Weisman, S.; Talmon, Y.; Barenholz, Y. *Crit. Rev. Ther. Drug Carrier Syst.* **2004**, *21*, 257-317.
- (100) Subramanian, M.; Holopainen, J. M.; Paukku, T.; Eriksson, O.; Huhtaniemi, I.; Kinnunen, P. K. J. *Biochim. Biophys. Acta* **2000**, *1466*, 289-305.
- (101) Wheeler, C. J.; Felgner, P. L.; Tsai, Y. J.; Marshall, J.; Sukhu, L.; Doh, S. G.; Hartikka, J.; Nietupski, J.; Manthorpe, M.; Nichols, M.; Plewe, M.; Liang, X.; Norman, J.; Smith, A.; Cheng, S. H. *Proc. Natl. Acad. Sci. U. S. A.* **1996**, *93*, 11454-11459.
- (102) Kinnunen, P. K. J.; Kõiv, A.; Lehtonen, J. Y. A.; Rytömaa, M.; Mustonen, P. *Chem. Phys. Lipids* **1994**, *73*, 181-207.
- (103) Gil, T.; Ipsen, J. H.; Mouritsen, O. G.; Sabra, M. C.; Sperotto, M. M.; Zuckermann, M. J. *Biochim. Biophys. Acta* **1998**, *1376*, 245-266.
- (104) Sackmann, E. In *Physical basis for trigger processes and membrane structures*. Chapman, D., Ed.; Biological membranes; Academic Press: London, 1984; Vol. 5, pp 105-143.
- (105) Mattjus, P.; Pike, H. M.; Molotkovsky, J. G.; Brown, R. E. *Biochemistry (N. Y.)* **2000**, *39*, 1067-1075.

- (106) Tuominen Esa, K. J.; Wallace Carmichael, J. A.; Kinnunen Paavo, K. J. *J. Biol. Chem.* **2002**, *277*, 8822-8826.
- (107) Säily, V. M. J.; Ryhänen, S. J.; Holopainen, J. M.; Borocci, S.; Mancini, G.; Kinnunen, P. K. J. *Biophys. J.* **2005**, *89*, 753.
- (108) Caldentey, J.; Hänninen, A.; Holopainen, J. M.; Bamford, J. K. H.; Kinnunen, P. K. J.; Bamford, D. H. *European Journal of Biochemistry* **1999**, *260*, 549-558.
- (109) Holopainen, J. M.; Angelova, M.; Kinnunen, P. K. J. *Meth. Enzymol.* **2003**, *367*, 15-23.
- (110) Angelova, M.; Dimitrov, D. *Faraday Discuss. Chem. Soc.* **1986**, *81*, 303-311.
- (111) Schnorf, M.; Potrykus, I.; Neuhaus, G. *Exp. Cell Res.* **1994**, *210*, 260-267.
- (112) Ryhänen, S. J.; Säily, M. J.; Paukku, T.; Borocci, S.; Mancini, G.; Holopainen, J. M.; Kinnunen, P. K. J. *Biophys. J.* **2003**, *84*, 578-587.
- (113) Scherer, P. G.; Seelig, J. *Biochemistry (N. Y.)* **1989**, *28*, 7720-7728.
- (114) Gurtovenko, A. A.; Patra, M.; Karttunen, M.; Vattulainen, I. *Biophys. J.* **2004**, *86*, 3461-3472.
- (115) Cardenas, M.; Nylander, T.; Joensson, B.; Lindman, B. *J. Colloid Interface Sci.* **2005**, *286*, 166-175.
- (116) Seelig, J.; Macdonald, P. M.; Scherer, P. G. *Biochemistry (N. Y.)* **1987**, *26*, 7535-7541.
- (117) Ryhänen, S. J.; Alakoskela, J. I.; Kinnunen, P. K. J. *Langmuir* **2005**, *21*, 5707-5715.
- (118) Zantl, R.; Baicu, L.; Artzner, F.; Sprenger, I.; Rapp, G.; Raedler, J. O. *J Phys Chem B* **1999**, *103*, 10300-10310.
- (119) Silviu, J. R. *Biochim. Biophys. Acta* **1991**, *1070*, 51-59.
- (120) Bandyopadhyay, S.; Tarek, M.; Klein, M. L. *J Phys Chem B* **1999**, *103*, 10075-10080.
- (121) Cevc, G. *Biochimica et Biophysica Acta, Reviews on Biomembranes* **1990**, *1031*, 311-382.
- (122) Manning, G. S. *Biophys. Chem.* **1978**, *9*, 65-70.
- (123) Boggs, J. M.; Moscarello, M. A.; Papahadjopoulos, D. *Biochemistry (N. Y.)* **1977**, *16*, 5420-5426.

- (124) Somerharju, P. J.; Virtanen, J. A.; Eklund, K. K.; Vainio, P.; Kinnunen, P. K. J. *Biochemistry (N. Y.)* **1985**, *24*, 2773-2781.
- (125) Clarke, R. J. *Adv. Colloid Interface Sci.* **2001**, *89-90*, 263-281.
- (126) Daune, M. In *Molecular Biophysics: Structures and Dynamics*. Section Title: General Biochemistry; 1999; , pp 499.
- (127) Hirko, A.; Tang, F.; Hughes, J. A. *Curr. Med. Chem.* **2003**, *10*, 1185-1193.
- (128) Kumar, V. V.; Chaudhuri, A. *FEBS Lett.* **2004**, *571*, 205-211.
- (129) Tang, F.; Hughes, J. A. *Bioconjug. Chem.* **1999**, *10*, 791-796.
- (130) Tang, F.; Hughes, J. A. *Biochem. Biophys. Res. Commun.* **1998**, *242*, 141-145.
- (131) Jong, L. I.; Abbott, N. L. *Langmuir* **2000**, *16*, 5553-5561.